




Article

Geoenvironmental Effects of the Hydric Relationship Between the Del Sauce Wetland and the Laguna Verde Detritic Coastal Aquifer, Central Chile

Blanca Gana ^{1,2}, José Miguel Andreu Rodes ³ , Paula Díaz ², Agustín Balboa ^{2,4}, Sebastián Frías ^{2,4}, Andrea Ávila ^{2,4}, Cecilia Rivera ^{2,5}, Claudio A. Sáez ^{2,5,6}  and Céline Lavergne ^{2,5,7,*} 

¹ Programa de Doctorado Interdisciplinario en Ciencias Ambientales, Universidad de Playa Ancha, Avenida Leopoldo Carvallo 270, Playa Ancha, Valparaíso 2340000, Chile; blanca.gana@upla.cl

² HUB Ambiental UPLA, Universidad de Playa Ancha, Valparaíso 2340000, Chile

³ Departamento Ciencias de la Tierra y del Medio Ambiente, Facultad de Ciencias, Universidad de Alicante, 03080 Alicante, Spain

⁴ Departamento de Geología, Facultad de Ingeniería, Universidad Nacional Andrés Bello, Viña del Mar 2520000, Chile

⁵ Departamento Ciencias y Geografía, Facultad de Ciencias Naturales y Exactas, Valparaíso 2340000, Chile

⁶ Departamento Ciencias del Mar, Facultad de Ciencias, Universidad de Alicante, 03080 Alicante, Spain

⁷ Departament de Biologia Marina i Oceanografia, Institut de Ciències del Mar (ICM), Consejo Superior de Investigaciones Científicas (CSIC), 08003 Barcelona, Spain

* Correspondence: lavergne@icm.csic.es

Abstract: In the central region of Chile, the Mega-Drought together with the demographic increase near the coast threatens groundwater availability and the hydrogeological functioning of coastal wetlands. To understand the hydric relationship between an aquifer and a wetland in a semi-arid coastal region of Central Chile (Valparaíso, Chile), as well as its geoenvironmental effects, four data collection campaigns were conducted in the wetland–estuary hydric system and surroundings, between 2021 and 2022, including physical, hydrochemical, and isotopic analyses in groundwater ($n = 16$ sites) and surface water ($n = 8$ sites). The results generated a conceptual model that indicates a hydraulic connection between the wetland and the aquifer, where the water use in one affects the availability in the other. With an average precipitation of 400 mm per year, the main recharge for both systems is rainwater. Three specific sources of pollution were identified from anthropic discharges that affect the water quality of the wetland and the estuary (flow from sanitary landfill, agricultural and livestock industry, and septic tank discharges in populated areas), exacerbated by the infiltration of seawater laterally and superficially through sandy sediments and the estuary, increasing salinity and electrical conductivity in the coastal zone (i.e., 3694 $\mu\text{S}/\text{cm}$). The Del Sauce subbasin faces strong hydric stress triggered by the poor conservation state of the riparian–coastal wetland and groundwater in the same area. This study provides a detailed understanding of hydrological interactions and serves as a model for understanding the possible effects on similar ecosystems, highlighting the need for integrated and appropriate environmental management.

Keywords: wetland; coastal aquifer; groundwater; hydrogeochemistry



Citation: Gana, B.; Rodes, J.M.A.; Díaz, P.; Balboa, A.; Frías, S.; Ávila, A.; Rivera, C.; Sáez, C.A.; Lavergne, C. Geoenvironmental Effects of the Hydric Relationship Between the Del Sauce Wetland and the Laguna Verde Detritic Coastal Aquifer, Central Chile. *Hydrology* **2024**, *11*, 174. <https://doi.org/10.3390/hydrology11100174>

Academic Editors: Yong Xiao, Jianping Wang and Jinlong Zhou

Received: 31 August 2024

Revised: 1 October 2024

Accepted: 8 October 2024

Published: 16 October 2024



Copyright: © 2024 by the authors. Licensee MDPI, Basel, Switzerland. This article is an open access article distributed under the terms and conditions of the Creative Commons Attribution (CC BY) license (<https://creativecommons.org/licenses/by/4.0/>).

1. Introduction

The groundwater connection to land surface processes and surface water bodies is multi-scale. These connections maintain flows along river corridors and into wetlands during droughts, ultimately resulting in continental river flow and its discharge to the oceans. These interactions across spatial scales close the hydrological cycle from the continent to the oceans in a dynamic balance [1]. Wetlands are surfaces covered by saline, brackish or fresh water, permanently or temporarily, artificially or naturally [2]. They have a high economic and social value due to the functions they perform, the goods that

can be obtained from them, and their attributes as a part of humanity's cultural heritage, although this has not always been the case. In the past, wetlands were considered unhealthy, dangerous, and economically worthless places, associated with diseases such as malaria due to the number of insects and other hydric diseases. This led to their misuse and abuse to the point of eliminating them. However, from a few decades ago, they began to be seen as areas of great diversity in plants and animals and given an important ecological and economic value. Thus, due to the dual effects of human activities and natural factors, the area of wetlands in the world has been decreasing and their quality has been deteriorating [3–9].

Many wetlands develop in places where groundwater is near the surface or are generally fed jointly by surface water and groundwater, with their water being a mixture of these two components [10]. Often, the aquifer status and the good condition of the wetland ecosystem are linked [11,12]. Therefore, the rational use of wetlands [13] requires that surface water, groundwater, and wetlands are managed in an integrated manner to ensure ecosystem and water sustainability. Hence, this requires an understanding of the interactions between groundwater and surface water, and therefore a robust hydrogeological framework [14].

Despite the strong dependence between groundwater and humid areas, the relationship between the wetland and the aquifer is often not known and this causes the use of groundwater to affect and deteriorate these damp environments. The use of groundwater for crop irrigation is one of the main problems suffered by aquifers. Overexploitation to extract water produces a drop in the water table and a decrease in the wetland contributions, especially during periods of low water levels when precipitation decreases. Moreover, water pollution in aquifers, for various reasons, especially by irrigation returns, can generate severe impacts in humid areas.

All this means that wetlands are among the most threatened ecosystems worldwide, in such a way that since 1900 more than 64% of the planet's wetlands have been lost, affecting the diversity of species present in these ecosystems [15]. From the study of wetlands of international importance, which integrates 2303 wetlands worldwide, Xu et al. [16] acknowledge that the most significant impact factors are pollution (54%), the use of biological resources (53%), modification of natural systems (53%), and agriculture and aquaculture (42%), with the wetlands' surfaces and environments being the most affected objects. Specifically, riverine wetlands are usually mainly affected by pollutants from domestic sewage, urban wastewater, garbage and solid waste, agricultural and forestry effluents, industrial effluents, etc., and are the most affected in terms of biodiversity and water resource regulations, while marine/coastal wetlands are the most vulnerable to climate change [16].

In Chile, knowledge about groundwater is quite limited and less than that available for other components of the hydrological cycle. This situation further complicates the understanding of the functioning and status of its humid areas. The lack of information on the distribution, quantity, and status of groundwater currently becomes more relevant due to the risk of hydric deficit [17]. According to the Intergovernmental Panel on Climate Change [18], the mean annual precipitation will decrease in mid and low latitudes by the end of the century [18–20], reducing the annual average river runoff and water availability [19], and will increase the sea level, which will extend the salinization of groundwater and estuaries, affecting water quality and further reducing the availability of fresh water for populations and ecosystems in coastal areas [19]. In the coastal basins of Central Chile (30°–38° S) in Southern Latin America, both surface and groundwater resources are highly dependent on rainy periods [21] and are therefore predicted to be under high water pressure. In this central area of Chile, there are diverse types of wetlands, such as high Andean meadows and temporary wetlands (stream ravines and streams) [22]. A large part of these wetlands has been affected since 2010 by a notorious decrease in precipitation, with annual deficits between 25% and 45%, generating a continuous dry period of several years that has been called The Central Chile Mega-Drought [23]. This deficit generated a decrease in

river flows, reservoirs, groundwater, and vegetation productivity in the northern sector of Central Chile [24], in addition to a decrease of up to 90% in average river discharge [25].

The Valparaíso Region, located in this area of Chile, and on which this study is focused, is a clear example of the climatic and demographic affectation, in which humid areas have begun to suffer. In 2021, accumulated precipitation as of June 30 reached about 100 mm at the Peñuelas Lake station, while a normal year (calculated for the 1991–2020 period) reaches 300 mm [26]. At the same time, a deficit in the flow levels of more than 45% was recorded [26]. The Laguna Verde sector (33°05' S–71°35' W) has faced significant anthropogenic pressure, particularly since 2010, due to rapid growth in the accommodation and tourism industries [27]. Additionally, the expansion of small-scale agriculture and potential industrial surface pollution also affected the Del Sauce stream [28], the main watercourse in the area. Consequently, the quality of this vital water resource has progressively declined [28–31]. However, the water from the estuary continues to be used for irrigation and recreational activities in the coastal zone, as recorded by DGA [32] and Tobar and Torres [33], and has been recognized in the summer period within the framework of this study.

This research responds to the socio-environmental problems of the Laguna Verde town (Valparaíso, Chile), and seeks to understand the relationship between groundwater and surface water of the Del Sauce stream, to identify its conservation status, the causes of this, and its possible geoenvironmental effects. Therefore, it is intended to advance, using knowledge of the groundwater in this region, an accurate definition of the aquifer or aquifers related to the Del Sauce stream, its geometry, typology, flow directions, its waters classification, and its interaction with the wetland. To achieve this goal, a holistic analysis was carried out covering hydrochemical, isotopic, piezometric, and physicochemical measurements in both groundwater and surface water, inside and outside the Del Sauce basin, during a full year of monitoring.

2. Methodology

2.1. Geographical Setting

The study area corresponds to the immediate surroundings of the Del Sauce stream, where the town of Laguna Verde is placed, located on the western margin of South America in Central Chile, and has been delimited approximately between UTM coordinates 6,337,500 N–6,327,500 N and 250,000 E–258,000 E. The town of Laguna Verde is considered a tourist center and is located approximately 9 km from the regional capital Valparaíso, which in the last census of 2017 had 3686 inhabitants.

The region is part of the Peñuelas Lake subbasin, defined within the so-called Coastal Basins between Aconcagua and Maipo [34]. According to the Chilean Ministry for the Environment, it is a continental, riparian, and permanent wetland type, which integrates the Las Cenizas and Del Sauce streams, called Del Sauce Estuary Wetland (<https://humedaleschile.mma.gob.cl/> (accessed on 10 July 2024); Figure 1). The Del Sauce stream, (also called El Sauce), which flows into the sea in the Laguna Verde Bay, emerges in the confluence area between the Las Cenizas and the La Luz streams [21] (sporadic contribution from the outflow of the La Luz lagoon that acts as a reservoir, which in return receives water from the Peñuelas Lake; Figure 1). Along the valley of the Del Sauce stream, there is a small detritic aquifer developing, of which waters are used to supply and irrigate the Laguna Verde locality.

The Laguna Verde region is affected by a Mediterranean climate with winter rainfall and coastal influence (Csb), according to the Köppen–Geiger climate classification, with average annual precipitation of 600 mm and average annual temperatures of 14 °C [35].

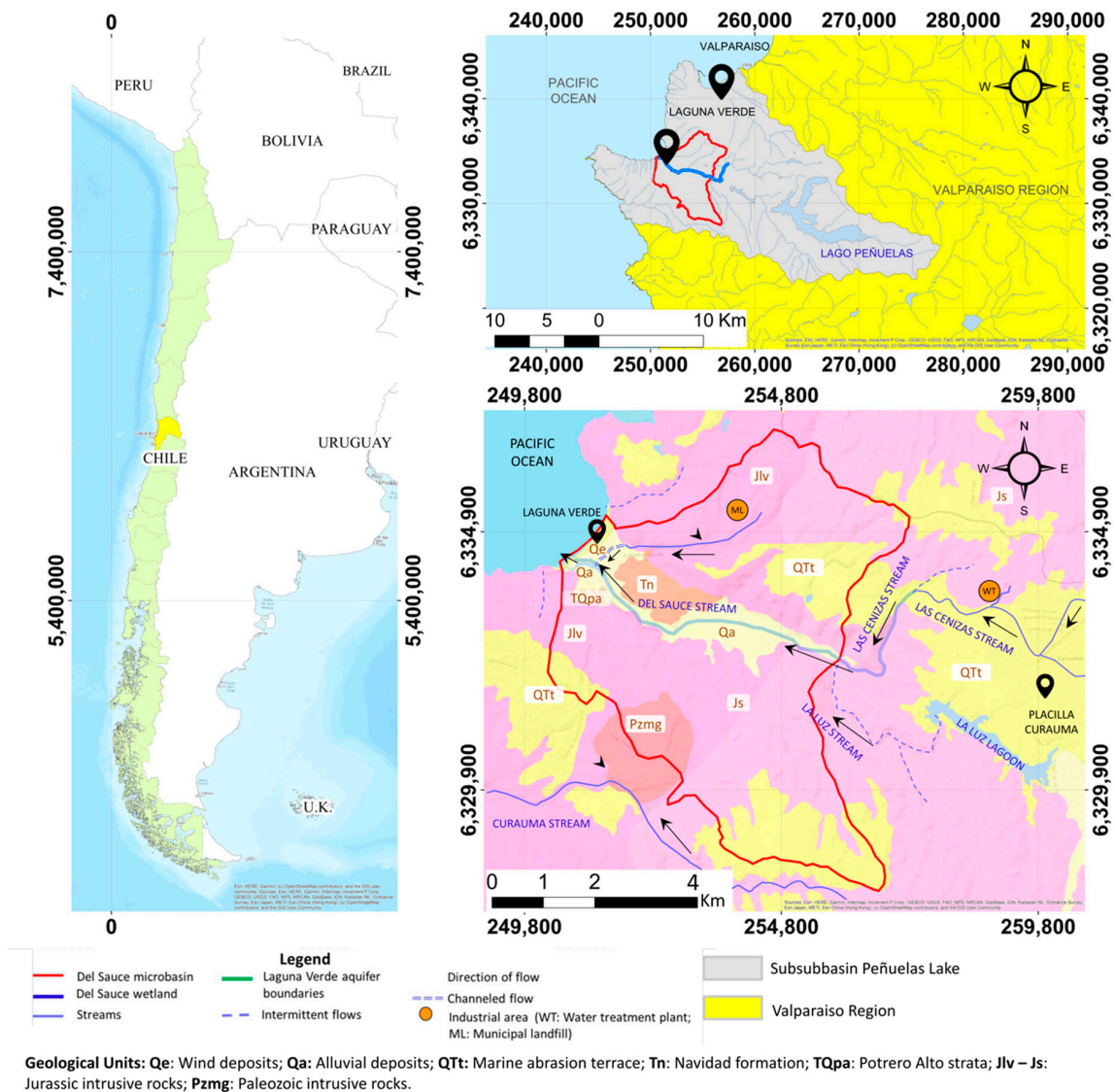


Figure 1. Map of the studied area: Left: Chile in South America and location of Valparaíso region (in yellow). Right–above: location of the Peñuelas Lake basin and the Del Sauce microbasin. Right–below: geologic map of the Del Sauce microbasin, hydrographic network with flow direction, highlighting the location of the Del Sauce wetland and industrial areas.

Upstream of the so-called Del Sauce wetland, in the locality of Placilla, the wastewater treatment plant, owned by the ESVAL company (UTM coordinates: 6,333,341 N and 259,360 E, Zone S19; Figure 1) treats wastewater generated in the localities of Placilla and Curauma (14,906 dwellings as of 2019) to be disposed in the Las Cenizas affluent, complying with the Chilean emission standard for the regulation of pollutants associated with liquid waste discharge to marine and inland surface waters, approved by the D.S. MINSEGPRES No. 90/00 [36]. The treatment consists of a roughing stage for the removal of the garbage that accompanies wastewater, then a stage of biological removal of the organic load in an aerated lagoon, to then move to a settling lagoon, in order to separate the biological sludge by assisted decantation, and finally a stage of effluent disinfection, treated with chlorine to remove the microbiological load, for subsequent disposal in the Las Cenizas affluent [36]. Another relevant industrial point in the basin under study corresponds to the El Molle sanitary landfill, which is called a treatment and final disposal center for household solid waste, solid waste assimilable to household, and hospital waste, designed to use a surface of 56.7 ha, and is placed in the same area of the former El Molle landfill, which covers a

surface of approximately 30 ha, covering between both projects a total of 86.1 ha of the El Molle property, located in the Quebrada Verde sector, Colorado Hill, in the coastal area of the Valparaíso Region (UTM coordinates: 254,703.5 N and 6,335,741.6 N, Zone S19).

2.2. Hydrological and Geological Setting

The region has an abrupt relief, with low altitudes where the Del Sauce stream flows, reaching between 1 and 20 m above sea level, surrounded by mountain ranges that rise up to 550 m above sea level (Figure 1). The Del Sauce stream basin has an area of 34.2 km², a perimeter of 29.87 km, a width of approximately 6 km, and is defined as a microbasin (according to the classification of Reyes et al. [37]). The compactness coefficient or Gravelius index provides a coefficient $K_c = 1.44$, indicating an average tendency to flooding (according to the classification of Villela and Matos [38]). The hypsometric curve of this microbasin compared with the curves proposed by Strahler [39] indicates that this basin represents a mature river, being in an intermediate stage, characterized by being in a state of equilibrium. The average slope of the basin reaches 19%, consequently, according to Alcántara's classification [40], it corresponds to a "Moderately steep" basin. The structure degree of the drainage network for the microbasin is of order "3", which with respect to the classification of the stream type determines a "medium" bifurcation degree [41].

From the geological point of view, most part of the Del Sauce basin is characterized by the presence of an intrusive basement, with rocks such as diorites, gabbros, and tonalites of Jurassic age, belonging to the Laguna Verde and Sauce units (Jlv and Js, respectively) [42,43]. In the middle and lower part of the Del Sauce stream, sedimentary rocks of Tertiary age are recognized, such as a relic of the Navidad Formation (Tn; Figure 1), which is made up of sandstones, shales, and siltstones, which have a maximum thickness of 120 m [44], and the Potrero Alto Strata (TQpa). As quaternary deposits, the so-called Abrasion Terrace (QTt) of marine origin are recorded in high sectors. The lower areas of the basin, where part of the Laguna Verde town is placed, are filled with unconsolidated sediments comprising fluvial deposits with interdigitated gravitational deposits, composed of medium sands, fine to medium gravels, and small portions of clays, forming the unit Alluvial Deposits of Holocene age (Qa) [43]; while bordering the coastline, there are unconsolidated beach sediments, composed of sands and gravels of well-rounded boulders that may form active dunes, and are defined as Current Littoral and Wind Deposits, of Holocene age (Qe; Figure 1) [43]. Structurally, the Laguna Verde fault stands out, corresponding to a tectonic fault of normal character, in an NW direction, with a sunken block toward the south (on which the channel of the Del Sauce stream is placed), which extends along the northern limit of the alluvial fill of the Del Sauce stream [43,45].

2.3. Hydrogeological Characterization

To define the hydrogeological units in the study area, after defining the drainage basin, a geological survey was generated. Subsequently, the hydraulic and stratigraphic background and pumping tests present in the records of the wells registered in the Chilean Ministry of Public Works, requested through the Chilean Law on Transparency at <http://www.portaltransparencia.cl> (accessed on 16 January 2024), were reviewed. To complete the information and obtain current data, two Porchet Tests were performed in the wetland (UTM coordinates 251,347 E; 6,334,158 N and 253,003 E; 6,333,071 N). These data were processed with the open-access AQTESOLV software version 4.0. Based on the geological characteristics of the study area and the permeability or hydraulic conductivity ranges obtained, the different geological formations were hydrogeologically characterized.

2.4. Flow Measurement

To determine the runoff flow in the Del Sauce stream, a gauging point was selected in the upper course of the river, specifically in the so-called Las Cenizas stream (sector S20). All this flow runs over the Del Sauce downstream until it reaches its final section before reaching the sea, where it remains dammed for most of the year by a sandbank, in such a

way that it does not discharge directly into the sea. During the campaigns carried out in the area (4 campaigns during the years 2021 and 2022), it was detected as the only estuary providing surface hydric resources. These measurements were performed with a Portable Hydraulic Winch (FP111, Global Water), according to the velocity–area method, or Bühler velocity–area method [46].

2.5. Piezometric Measurement

Piezometric levels were measured in reachable wells, corresponding to 9 wells constructed in the Alluvial Deposit unit (P1, P3, P5, P6, P7, P8, P10, P14, P15), one in the unit Current Littoral and Wind Deposits (P4), one in the Navidad Formation (P2), one in the unit Potrero Alto strata (P26), one in the unit Abrasion Terrace (P27), and two in the Jurassic Intrusives unit (P12 and P13; Figure 2). These measurements were carried out with a 100 m water level meter (Holykell brand). From these measurements, isopiestic maps were generated to establish the flow direction, thus defining groundwater dynamics. Based on the geographic density, an equidistance of 1 m was defined between each piezometric curve.

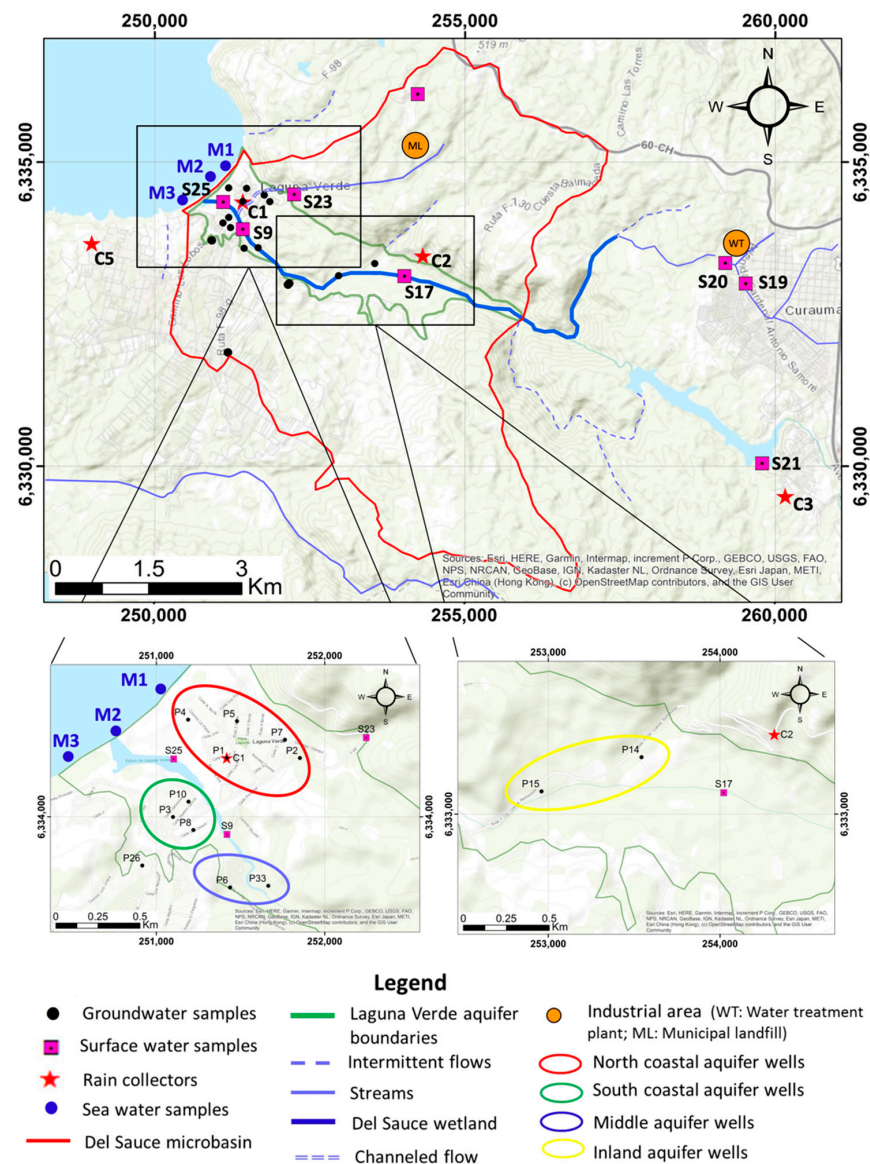


Figure 2. Location of sampling sites and physicochemical data collection: Above: location map of the study area and sampling points for surface water, groundwater, and rainwater collectors. Below–left: details of the coastal and middle zone; below–right: details of the inland zone.

2.6. Water Sampling

To characterize the surface water and groundwater chemistry in the studied area and establish the hydric relationship of groundwater with the Del Sauce stream, four field campaigns were conducted. Water was sampled for the physicochemical and isotopic analysis. Sampling was carried out during the months of September–October 2021 (spring), January–February 2022 (summer, dry season), April–May 2022 (autumn), and July–August 2022 (winter, rainy season).

The hydrogeochemical sampling points selected corresponded to groundwater ($n = 16$) collected from wells located in the different geological units of the study area, and surface water ($n = 8$), collected from La Luz Lagoon, Del Sauce stream, Las Cenizas affluent, spring in the upper part adjacent to the sanitary landfill site, and surface runoff from this same industrial area. In addition, during the winter and spring 2022 campaigns, three seawater samples were collected in the northern, middle, and southern zones of the bay (M1, M2, and M3, respectively; Figure 2). At each selected point, pH, total dissolved solids (TDS), temperature, dissolved oxygen (DO), water electrical conductivity (EC), and chemical oxygen demand (COD) were measured in situ with a portable multiparameter meter (HI98194, Hanna) as well as free chlorine with a chlorine meter (Pocket Colorimeter II, HACH). Turbidity was measured with a turbidimeter (HI83414, Hanna) and color was evaluated by visual comparison (St. Method 2120B; Table S1). Water samples were taken in triplicate to be analyzed by major ions (calcium, magnesium, sodium, potassium, chloride, sulfate, bicarbonate) and other secondary ions (such as nitrites, nitrates, phosphates, carbonates, and fluorides), microelements (such as aluminum, bromide, manganese, lead, among others) and microbiological elements (fecal and total coliforms). The elements boron and strontium were measured in one sample from the sea, one from the coastal aquifer, one from the inland aquifer, and one from the estuary at its mouth, for the last two sampling campaigns. All analyses were performed following the methodologies proposed in the 24th Edition of *Standard Methods for the Examination of Water and Wastewater* (details available in Supporting Materials, Table S1).

For the first season sampling (spring: September–October 2021), 25 samples were selected for the ^2H and ^{18}O water isotopic analyses in triplicates and 5 rainwater collectors were arranged in a transect from the lower to the upper part of the basin (samples C1 to C5; Figure 2). During the following field campaigns (summer, autumn, and winter of 2022), all hydrogeochemical sampling points were considered for isotopic analysis. These samples were sent for ^2H and ^{18}O water isotope analysis to the Alfred Wegener Institute for Polar and Marine Research in Potsdam, Germany.

2.7. Data Analysis

For the morphometric, hydrogeological, and hydrodynamic analysis (flow model), as well as for the preparation of thematic maps, ArcMap 10.4 software was used. Regarding the hydrogeochemical information, the data were examined and analytically treated individually and in groups, in order to detect possible pollutant sources and the chemical relationship between groundwater and wetland in their different sections. The data groups correspond to the following (Figure 2): north coastal aquifer (wells P1, P2, P4, P5, P7); south coastal aquifer (wells P3, P8, and P10), middle aquifer (wells P6 and P33), and inland aquifer (wells P14 and P15). A multivariate analysis of variance (MANOVA) was performed to identify the factors that most influenced the physicochemical parameters and major ions. The free-access software Diagrammes (v 6.77) was used. To determine the irrigation water quality, the Riverside diagram [47] and Chilean Standard 1333 [48], which sets out the water quality requirements for different uses, were used. In turn, water–rock interactions and the study of hydrogeochemical processes or pollution problems were established using hydrogeochemical diagrams, such as modified Stiff Diagram [49], or Piper Diagram [50], and the ionic relations $r\text{Cl}^- / r\text{HCO}_3^-$, $r\text{SO}_4^{2-} / r\text{Cl}^-$, $r\text{Br}^- / r\text{Cl}^-$, $r\text{Mg}^{2+} / r\text{Ca}^{2+}$, $r\text{K}^+ / r\text{Na}^+$, and $r\text{Na}_2^+ / r\text{Cl}^-$ [51–53].

For the isotopic analysis of both surface water and groundwater, the $\delta^{18}\text{O}$ ‰ v/s $\delta^2\text{H}$ ‰ V SMOW diagrams were used, performed with the software Diagrammes (v 6.77).

3. Results

3.1. Precipitation and Flows

The average annual precipitation in the Del Sauce region had great variability during the years 2010 and 2022, years that are considered within the so-called Mega-Drought in Central Chile (CR2, 2015). According to data from the meteorological directorate of Chile, the average precipitation measured in the study area surroundings (Peñuelas Lake weather station: UTM coordinates 6,329,722 N and 261,586 E, Zone S 19), for a range of 30 years (1992–2022), reached an annual average of 585 mm, while the precipitation recorded for the range of the years between 2010 and 2022 (range within Mega-Drought) reached an annual average of 406 mm, which represents a 30% decrease in precipitation of the area in relation to a normal year. Within the period called Mega-Drought, in the study area, a maximum annual precipitation of 677 mm was recorded in 2015, and a minimum of 129 mm in 2019. Regarding precipitation distribution over an average year, the maxima are recognized mainly during the austral winter in the months of June, July, and August, with average values of 127 mm, followed by the month of May of the autumn mid-season, with an average of about 100 mm, while the minimum precipitation records are recognized in the months of January, February, and March, corresponding to the dry summer season, with seasonal averages of 1.9 mm, determining that the study area corresponds to a Unimodal precipitation regime (Figure 3).

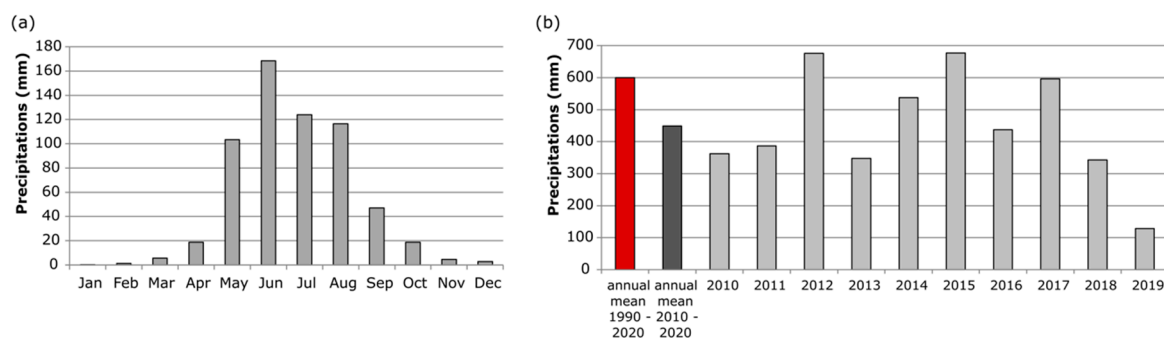


Figure 3. Average precipitation in the studied area: (a) monthly average precipitation for the period 1992–2022. (b) annual average precipitation for the periods 1992–2022 (red), 2010–2022 (dark gray), and detail of annual precipitation for each year between 2010 and 2022 (light gray).

Regarding Del Sauce stream hydrometry, the flow measured in the summer dry season (March 2022) reached $0.2 \text{ m}^3/\text{s}$, and $0.32 \text{ m}^3/\text{s}$ in the winter rainy season (August 2022), estimating an average annual flow for the Del Sauce wetland of $0.26 \text{ m}^3/\text{s}$.

3.2. Hydrogeology

Until now, the only hydrogeological information of the study area resided in the reports conducted by the DGA (2017) [54] in which this zone was included within the so-called Laguna Verde Estuary aquifer that comprises a large part of the Peñuelas Lake basin that extends inland toward the continent from the Pacific Ocean to approximately 27 km in a SE direction. Under this definition, the Peñuelas Lake basin comprises a basin surface of 204 km^2 , and an aquifer area of 43.8 km^2 (Figure 1).

Particularly, in the Del Sauce microbasin, based on the geological and hydrogeological review carried out, two sets of varied lithologies have been defined that can be considered as independent units with clearly different hydrogeological behavior (Figure 4).

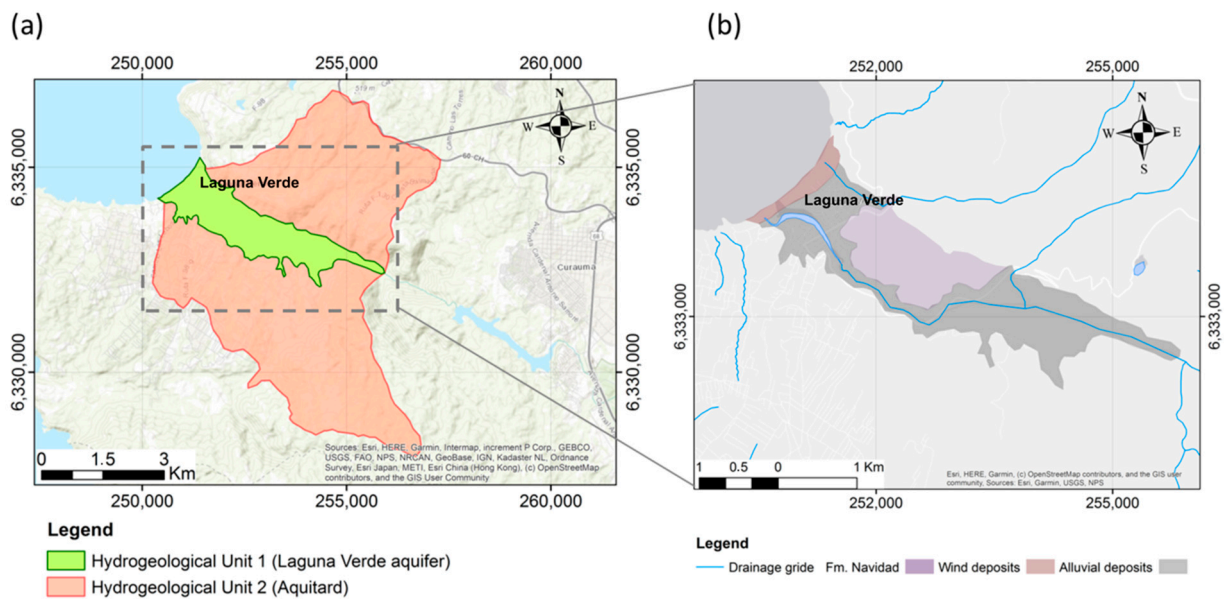


Figure 4. (a) Hydrogeological units in the Del Sauce microbasin. (b) Details of geological units of HU1.

Hydrogeological Unit 1 (HU1): Denominated in this study as Laguna Verde Detritic Coastal Aquifer or Laguna Verde Aquifer. This is a detritic aquifer formed mainly by alluvial sediments such as medium sands and fine to medium gravels with small portions of clays, belonging to the Alluvial Deposits formation [43] that fill the valley of the Del Sauce; by poorly consolidated detritic rocks that constitute the Navidad Formation located on the northern edge of the valley, with a maximum depth of 120 m [44]; and by quaternary wind sediments (coarse-to-medium sands), which form a small strip of approximately 200 m from the coastline inland, and are called Wind Deposits Unit [43]. Thus, the Laguna Verde Detritic Coastal Aquifer reaches a total area of 5 km², and a perimeter of 16,668 m. The aquifer thickness is not known exactly, since most of the points do not reach the impermeable wall. According to the information obtained in this study based on the constructive characteristics of the existing wells, everything indicates that it would present a minimum of 10 m in the coastal zone and 25 m in the inland zone. According to information from some aquifers in adjacent coastal basins with similar characteristics, these small coastal aquifers have a maximum thickness of 30 m [34]. This unit acts as a free detritic aquifer.

The hydraulic characterization of this unit, transmissivity (T) and permeability (k), has been made from the reinterpretation of pumping tests for the geological units. In the Alluvial Deposits, it has been determined that T reaches an average of 200 m²/day. Considering an approximate saturated thickness of 20 m, the permeability (k) obtained was 10 m/day. Locally, the two Porchet tests performed for this study in this unit revealed an infiltration rate of 124 and 194 mm/h, corresponding to a permeability $k = 3$ and 4.7 m/day, respectively. In the Navidad Formation, a transmissivity of 195 m²/day and a permeability of 7.8 m/day were measured, considering an approximate saturated thickness of 25 m. These results indicate that both lithological sections have good hydrogeological characteristics and constitute a good aquifer.

Hydrogeological Unit 2 (HU2): Defined by the Jurassic intrusive rock units (grouping the Laguna Verde and Sauce geological units), which in the study area are recognized as highly weathered and with a high clay content, with estimated permeabilities based on their granulometry close to 10⁻⁷ m/s. In addition, this unit includes the unit Abrasion Terrace, corresponding to high marine terraces located on the crystalline rocks, the unit Potrero Alto Strata, and Paleozoic intrusives. Although in this unit there are home extraction wells, the difficulty of these wells to contain and provide significant or enough water volumes throughout the year is also recognized. The catchments in this unit presented very

depressed piezometric levels, and in many of them, when water was extracted for sampling, these dried up, which shows the low productivity of the catchments. This hydrogeological unit corresponds to a very poor aquifer or aquitard.

3.3. Heads and Relation between Stream and Aquifer

Based on the piezometric levels, the dynamics of groundwater flow in the Laguna Verde aquifer were analyzed. Broadly speaking, the isopiestic maps elaborated for the dry and humid seasons suggest a certain similarity in the behavior throughout the year (Figure 5a,b). The flow of the aquifer waters has a general direction from the southeast, which corresponds to its highest part, toward the northwest, where the discharge into the sea occurs.

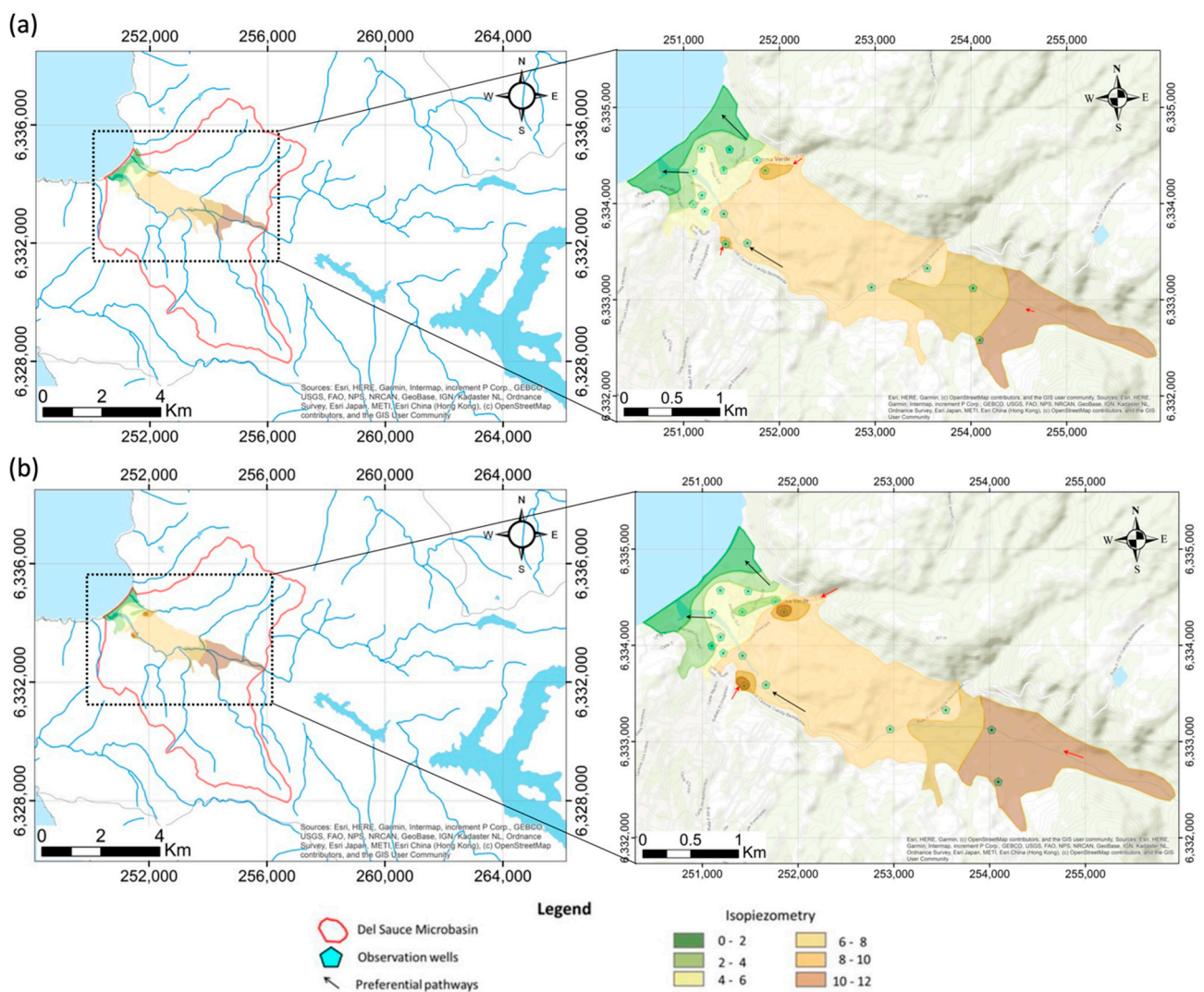


Figure 5. (a) Location of the Laguna Verde aquifer, with details of the Piezometric map for summer 2022 (December to March, austral dry season). (b) Location of the Laguna Verde aquifer, with details of the Piezometric map winter 2022 (June to August, austral rainy season) isopiestic every 1 m. Red arrows indicate recharge zones to the Laguna Verde aquifer.

A piezometric threshold in the coastal zone stands out, where higher levels are reached in the sector where the Del Sauce stream flows, which is maintained over time, resulting in a groundwater divide that would separate the northern and the southern sectors.

Three sectors were recognized with high piezometric altitudes throughout the year. The most relevant in the interior zone of the aquifer, in the headwaters of the basin, with altitudes above 10 m a.s.l., a second sector of smaller extension, recorded in well P2, and the third in the middle sector recorded in well P6, both with piezometric altitudes above 8 m a.s.l.

3.4. Hydrogeochemistry of the Hydrological System

3.4.1. Physicochemical Parameters

Details of the physicochemical parameters of the hydrological system under study are presented in Table 1. The annual average of total dissolved solids (TDS) in the waters of the Del Sauce and Las Cenizas streams reaches 920 mg/L, and increases downstream, recording 652 mg/L in the upper zone S20, until reaching 1263 mg/L in the lower Sauce or mouth. The TDS in the Laguna Verde aquifer has a spatially varying distribution, with 457 mg/L in the inland zone, passing through the middle zone with 633 mg/L, to the coastal or discharge zone, where it reaches 2173 mg/L, a behavior similar to the one presented by electrical conductivity (EC) in the zone. According to the Freeze and Cherry [55] classification, the waters from the north and southern coastal aquifer are classified as brackish (>1000 mg/L TDS). On the other hand, the artificial lagoon S30 and the dump flow S23 present annual averages of 10,567 and 6144 mg/L, respectively. The waters of HU2 reach 657 mg/L.

The pH in the waters of the Del Sauce and Las Cenizas streams ranged between 6 and 8.4, with an annual average of 7.6, while groundwater has a pH between 6.8 and 7.2, with an average of 7. The waters of the lagoon adjacent to the sanitary landfill in the upper sector of the basin (S30) and of the dump flow from the same sector (S23) have an annual average pH of 6.5 and 8.1, respectively. On the other hand, the groundwater that characterizes Hydrogeological Unit 2 (HU2) has an annual average pH of 7.4.

3.4.2. Major and Relevant Ions

Table 1 shows concentrations of the major ions and recommended ones in the waters of the study. During the studied period, Las Cenizas (S20) was the unique affluent feeding the Del Sauce stream. In this sampling site, the major ion is bicarbonate (271 mg/L), with values similar to those found in the upper section of the Del Sauce stream (224 mg/L). In its middle and lower sections, chloride becomes predominant in the wetland waters (329 and 440, respectively). The predominant ion in the inland zone of the aquifer is bicarbonate (159 mg/L), a composition similar to that of the middle zone (159 mg/L), with the difference that there is an increase in chloride ions, from 69 mg/L in the inland zone to 124 mg/L in the middle zone, with the latter ion becoming predominant in the coastal zone of the aquifer (807 mg/L). The samples from the flow coming from the sanitary landfill (S23) have annual averages of chloride and sulfate of 1987 y 1640 mg/L, respectively, while in the lagoon S30, sulfate predominated with 2179 mg/L. On the other hand, HU2 waters present similar concentrations between bicarbonate (166 mg/L), chloride (168 mg/L), and sulfate (106 mg/L) ions.

Nitrates show an annual average of 6.5 mg/L in the Las Cenizas affluent, 13.3 mg/L in the upper section of the Del Sauce stream, 9.4 mg/L in its middle section, and 9.7 mg/L in its lower section. Low nitrate concentration was detected in groundwaters from the inland sector. In its middle section, nitrates in the aquifer reach an annual average of 2.3 mg/L, with the highest concentration in the southern coastal sector with 64 mg/L, followed by the north coastal sector with 51 mg/L. The artificial lagoon S30 presents an annual average concentration of this ion of 21.2 mg/L, while the dump flow S23 reaches the highest concentration of nitrates in the hydric system with 155 mg/L. The nitrates present in HU2 reach 34.5 mg/L.

Table 1. Concentrations of the major ions and recommended ones in the waters of the study area (mean \pm SD mg/L) and annual average and standard deviation of physicochemical parameters measured in situ in the study area. TDS: total dissolved solids; T: temperature; EC: electrical conductivity; OD: oxygen demand; COD: Chemical Oxygen Demand; TUR: turbidity; COL: color.

		Major Ions and Recommended										Physicochemical Parameters							
	Parameters	HCO ₃ ⁻ mg/L	CO ₃ ²⁻ mg/L	Cl ⁻ mg/L	SO ₄ ²⁻ mg/L	Na ⁺ mg/L	K ⁺ mg/L	Mg ²⁺ mg/L	Ca ²⁺ mg/L	NO ₃ ⁻ mg/L	NO ₂ ⁻ mg/L	TDS (mg/L)	T (°C)	pH	EC (μ S/cm)	DO (mg/L)	COD (mg/L)	TUR NTU	COL Pt-Co
Groundwater	North coastal aquifer	219 \pm 44	0.5 \pm 0.9	854 \pm 469	424 \pm 327	149 \pm 146	10.5 \pm 6	94 \pm 81	114 \pm 98	51 \pm 55	0.6 \pm 0.1	2493 \pm 1094	15.5 \pm 1.3	6.8 \pm 0.5	4155 \pm 2044	3.6 \pm 2.1	31.2 \pm 26.2	1.0 \pm 1.1	12.8 \pm 8
	Southern coastal aquifer	162 \pm 39	0.1 \pm 0.1	761 \pm 666	185 \pm 108	219 \pm 279	14.8 \pm 4.5	55 \pm 26	80 \pm 28	64 \pm 86	0.3 \pm 0.6	1853 \pm 1186	16.3 \pm 1.2	6.9 \pm 0.4	2925 \pm 2211	5.2 \pm 1.4	8.0 \pm 5.8	1.4 \pm 2.3	5.4 \pm 1.5
	Middle aquifer	159 \pm 30	0.7 \pm 1.4	124 \pm 46	99 \pm 68	54 \pm 24	2.1 \pm 0.4	27 \pm 10	30 \pm 14	24 \pm 36	0.2 \pm 0.3	633 \pm 142	16.5 \pm 0.9	7.2 \pm 0.6	1309 \pm 462	6.6 \pm 2	3.6 \pm 5.1	17.2 \pm 23.6	4.8 \pm 1.5
	Inland aquifer	159 \pm 30	0.3 \pm 0.3	69 \pm 9	60 \pm 29	59 \pm 59	1.7 \pm 0.9	36 \pm 30	67 \pm 74	1.3 \pm 1.5	0.01 \pm 0	4577 \pm 200	16.3 \pm 0.3	7.2 \pm 0.6	643 \pm 172	4.2 \pm 2.5	2.2 \pm 2.8	7.9 \pm 12.4	10.6 \pm 15.9
	HU2	166 \pm 48	0.4 \pm 0.3	168 \pm 75	106 \pm 67	71 \pm 35	4.6 \pm 3	32 \pm 1	40 \pm 20	35 \pm 57	0.2 \pm 0.2	657 \pm 230	16.9 \pm 1.9	7.4 \pm 0.7	1134 \pm 291	6.2 \pm 2.2	2.7 \pm 3.5	5.4 \pm 11.3	6.7 \pm 9.2
Surface Water	La Luz Lagoon	108 \pm 6	5.1 \pm 8.6	34 \pm 3	28 \pm 1	41 \pm 35	2.2 \pm 1.2	37 \pm 46	131 \pm 199	3 \pm 2.9	0.02 \pm 0	229 \pm 44	16.4 \pm 4.9	8.3 \pm 0.6	405 \pm 26	7.8 \pm 2.8	44.6 \pm 59.6	4.5 \pm 2.8	6.3 \pm 2.5
	Las Cenizas (S19)	287 \pm 50	1.1 \pm 0.7	101 \pm 31	183 \pm 24	56 \pm 24	6.25 \pm 5.5	31 \pm 9	71 \pm 17	24 \pm 33	0.1 \pm 0	637 \pm 75	14.2 \pm 4.3	7.4 \pm 0.5	1213 \pm 288	5.6 \pm 3.9	91.7 \pm 62.7	22 \pm 16.8	29 \pm 24.6
	Las Cenizas (S20)	271 \pm 23	0.5 \pm 0.3	137 \pm 58	162 \pm 23	59 \pm 28	16.7 \pm 1.3	20 \pm 5	72 \pm 23	6.5 \pm 6	0.1 \pm 0.02	652 \pm 139	16.6 \pm 4.8	7.2 \pm 0.4	1124 \pm 288	5.9 \pm 1.7	61.5 \pm 31.7	16.6 \pm 10.1	17.5 \pm 5
	High El Sauce	224 \pm 44	2.9 \pm 2.8	155 \pm 17	155 \pm 25	62 \pm 28	17.4 \pm 2.3	22 \pm 6	75 \pm 23	13 \pm 11	3.4 \pm 0.5	702 \pm 227	12.8 \pm 2.6	7.9 \pm 0.4	1429 \pm 624	5 \pm 2.8	58.2 \pm 26.2	14.0 \pm 7.4	15.0 \pm 5.8
	Middle El Sauce	187 \pm 62	1.6 \pm 1.2	329 \pm 125	185 \pm 29	134 \pm 98	18 \pm 3.4	33 \pm 11	66 \pm 13	9.4 \pm 8.5	2.6 \pm 2.6	1064 \pm 327	16.14 \pm 2.4	5.9 \pm 3.8	1831 \pm 562	8.1 \pm 2	57.6 \pm 28	13.2 \pm 9.1	18.8 \pm 2.5
	Lower El Sauce	171 \pm 48	3 \pm 2.2	440 \pm 222	189 \pm 36	119 \pm 126	20 \pm 3.4	37 \pm 12	63 \pm 15	9.7 \pm 6	8.02 \pm 7.1	1263 \pm 539	15.2 \pm 5.2	7.8 \pm 0.3	2279 \pm 1108	8.2 \pm 1.7	62.2 \pm 37.9	16.6 \pm 9.8	15.0 \pm 5.8
	Artificial Lagoon S30	11 \pm 5	0 \pm 0	6388 \pm 376	2179 \pm 2000	186 \pm 192	69 \pm 56	74 \pm 32	90 \pm 35	21 \pm 24	0.3 \pm 0.4	10,567 \pm 2263	15.3 \pm 3.5	6.5 \pm 3.5	15,532 \pm 2503	7.2 \pm 1	223.9 \pm 112.7	39 \pm 1.7	30 \pm 5.4
	Dump Flow S23	356 \pm 116	3.7 \pm 3	1987 \pm 344	1640 \pm 421	88 \pm 12	34 \pm 15.5	90 \pm 44	111 \pm 25	155 \pm 144	10.7 \pm 13.6	6144 \pm 1567	11.9 \pm 1.7	8.1 \pm 0.4	8552 \pm 1172	7.8 \pm 0.7	248.3 \pm 56.1	10.3 \pm 0.3	113 \pm 25.5

Regarding the hydrochemical facies identified by the Piper diagrams for surface water, it can be established that, in general, the waters in the Las Cenizas affluent have clear mixed facies with respect to cations and anions, while in the Del Sauce stream, they are of chloride and mixed types with respect to cations. On the other hand, the waters of the La Luz lagoon, located in the eastern part of the study area, are of the bicarbonate type, while they vary between calcic and mixed with respect to cations (Figure 6).

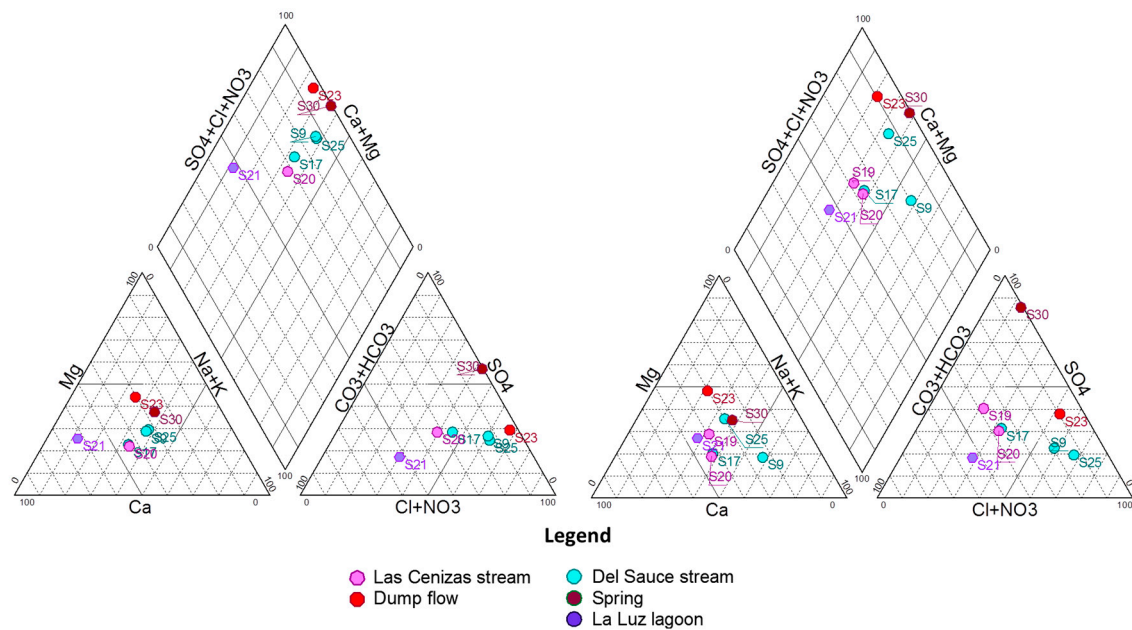


Figure 6. Piper diagrams for surface water of the study area in summer 2022 (left) and winter 2022 (right).

Regarding the other surface sources sampled, the artificial lagoon S30 and the dump flow S23 correspond to sulfate- and chloride-type waters, respectively, a condition that is maintained during the entire year (Figure 6).

Regarding the aquifer waters (Figure 7), mixed chloride and sodium facies are generally observed. However, during spring, the waters in the north coastal (P1) and southern coastal (P3 and P10) sectors are characterized by a sodium chloride water type. In winter, this tendency is observed more locally at points P10 and P33.

As shown in the modified Stiff diagram, the maximum mineralization was reached in spring 2021, while the lowest mineralization was recorded in summer 2022. As a tendency, mineralization gradually increased from summer to winter 2022 (Figure 7).

From the microelements analysis carried out in the waters of the entire hydric system studied (Table 2), the high value of Br stands out for surface water, where this element was highest downstream, reaching the lower Sauce area with concentrations of 7 mg/L. In groundwater, the presence of the minor constituents Al, Ba, Br, Fe, and Mn is observed with higher annual average concentrations than expected (>0.1 mg/L), highlighting the presence of Br, mainly in the north coastal zone, reaching concentrations of 18 mg/L. The inland zone presents concentrations of 1.8 mg/L of Br and 1.3 mg/L of Fe, while in the middle sector, both elements increase to 3.1 and 3.2 mg/L, respectively. In the runoff from the sanitary landfill (S23), Br reaches the highest concentration of the entire hydric system with 59.4 mg/L exhibiting high seasonal variability. On the other hand, the artificial lagoon S30 presents average Br concentrations of 12 mg/L, in addition to 4.5 mg/L of Al and 14 mg/L of Mn. In HU2 waters, the presence of Br (i.e., 3 mg/L) and Fe (i.e., 2 mg/L) stands out. The annual averages of the microelements omitted in the table (B, Cd, Li, Mo, Ni, Pb, Ag) had concentrations below the detection limit in all samples (<0.01 mg/L).

Table 2. Analysis of microelements in waters of the studied hydric system.

Microelements (mg/L)		F	Al	Ba	Br	Co	Cu	Fe	Mn	V	Zn
Groundwater	North Coastal aquifer	0.2 ± 0.03	0.7 ± 2.4	0.1 ± 0.03	17.9 ± 12.7	0.01 ± 0.001	0.03 ± 0.03	0.5 ± 1.4	1.1 ± 1.6	0.1 ± 0.1	0.03 ± 0.03
	Southern Coastal aquifer	0.2 ± 0.02	0.6 ± 1.5	0.1 ± 0.01	11.5 ± 9.5	0.008 ± 0.004	0.01 ± 0.005	0.2 ± 0.2	0.01 ± 0.007	0.06 ± 0.03	0.03 ± 0.02
	Middle aquifer	0.2 ± 0.05	0.1 ± 0.1	0.04 ± 0.02	3.1 ± 0.8	0.01 ± 0.00	0.04 ± 0.06	3.2 ± 4.7	0.3 ± 0.5	0.1 ± 0.1	0.03 ± 0.03
	Inland aquifer	0.2 ± 0.03	0.2 ± 0.3	0.1 ± 0.1	1.8 ± 1	0.1 ± 0.1	0.02 ± 0.02	1.3 ± 1.3	0.6 ± 1.3	0.01 ± 0.004	0.04 ± 0.05
	UH2	0.3 ± 0.1	0.8 ± 2.4	0.02 ± 0.02	3.0 ± 1.2	0.009 ± 0.003	0.02 ± 0.02	1.9 ± 5.8	0.04 ± 0.05	0.02 ± 0.01	0.04 ± 0.04
Surface Water	La Luz Lagoon	0.19 ± 0.0	0.77 ± 0.5	0.27 ± 0.4	0.83 ± 0.1	0.48 ± 0.8	0.04 ± 0.1	2.47 ± 3.5	0.1 ± 0.1	0.01 ± 0.0	0.021 ± 0.0
	Las Cenizas S19	0.46 ± 0	2.2 ± 2.8	0.05 ± 0.01	1.1 ± 0	0.01 ± 0.01	0.01 ± 0.01	2.3 ± 2.6	0.62 ± 0.3	0.02 ± 0.01	0.03 ± 0.01
	Las Cenizas S20	0.45 ± 0.06	0.64 ± 0.16	0.02 ± 0	1.94 ± 0.7	0.01 ± 0.01	0.24 ± 0.4	2.13 ± 0.2	0.2 ± 0.06	0.01 ± 0	0.07 ± 0.09
	High El Sauce	0.4 ± 0.03	0.5 ± 0.3	0.03 ± 0.005	3.0 ± 0.9	0.007 ± 0.00	0.1 ± 0.1	1.2 ± 0.3	0.3 ± 0.1	0.01 ± 0.0	0.04 ± 0.006
	Middle El Sauce	0.4 ± 0.06	1.6 ± 3.04	0.04 ± 0.006	5 ± 2.5	0.008 ± 0.004	0.03 ± 0.03	1.1 ± 1	0.6 ± 0.3	0.01 ± 0.0	0.01 ± 0.06
	Lower El Sauce	0.4 ± 0.1	0.9 ± 0.3	0.04 ± 0.0	7 ± 3.6	0.01 ± 0.001	0.03 ± 0.00	1.2 ± 0.2	0.6 ± 0.2	0.01 ± 0.0	0.01 ± 0.0
	Artificial Lagoon S30	0.2 ± 0.03	4.5 ± 0.01	0.1 ± 0.005	12.2 ± 0.7	0.01 ± 0.001	0.03 ± 0.00	2.5 ± 0.3	13.9 ± 3.6	0.2 ± 0.1	0.04 ± 0.009
	Dump Flow S23	0.1 ± 0.02	0.2 ± 0.01	0.1 ± 0.02	59.4 ± 13.5	0.01 ± 0.001	0.01 ± 0.00	0.9 ± 0.00	4.1 ± 0.3	0.4 ± 0.2	0.01 ± 0.0

3.4.3. Biological Contamination and Water Quality

Fecal coliforms were detected in all the groundwater samples from the coastal zone, with a particularly high abundance in the P4 well with >2400 MPN/100 mL. Fecal coliforms were also retrieved in the surface water of the artificial lagoon S30 (>2300 MPN/100 mL), in the flow from the sanitary landfill (S23) and at the mouth of the Del Sauce estuary, suggesting that these waters are limited for certain uses and crops.

In comparative terms and based on multiple indicators that include salinity, EC, TDS, Cu, V, and the presence of fecal coliforms, the best water quality for irrigation is recognized in La Luz Lagoon and in waters of the inland part of the aquifer, while the least recommended would be the waters of the north coastal part of the aquifer, those of well P10 (southern coastal aquifer), the waters of the artificial lagoon (S30), and those of the flow from sanitary landfill (S23).

3.4.4. Ionic Ratios

To establish the hydrogeochemical processes occurring in the Del Sauce stream and the interrelationship between the different surface waters and groundwaters, some ionic ratios, such as $rCl/rHCO_3$, rMg/rCa , rK/rNa , rBr/rCl , and rNa/rCl , were calculated for each of the established water subgroups (Figure 8).

Since this is a coastal system, the influence of seawater may have some significance; therefore, ionic relations were determined for the seawater of Laguna Verde Bay. The annual mean values obtained were $rCl/rHCO_3 = 297$; $rMg/rCa = 5.9$; $rK/rNa = 0.02$; $rBr/rCl = 0.03$; and $rNa/rCl = 0.84$. The spills and HU2 were also characterized. In the flow S23, the ratios calculated for summer and winter were $rCl/rHCO_3 = 19.3$ and 5.6; $rMg/rCa = 1.5$ and 1.6; $rK/rNa = 0.29$ and 0.22; $rBr/rCl = 0.01$ and 0.02; and $rNa/rCl = 0.07$ and 0.08, respectively, all indicating some variability of the effluent salinity over time. Regarding HU2, these relations are much lower and show some stability. In the Del Sauce stream, it can be noted that the $rCl/rHCO_3$ and rMg/rCa ratios increase from the upstream until the downstream section. This situation is similar between summer and winter.

Regarding the inland aquifer, it shows low values representative of freshwater in which mineralization is predominantly acquired by rock dissolution. However, groundwaters from the coastal part exhibit a greater variability. Interestingly, the highest rMg/rCa ratio (i.e., 1.84) was calculated in the P4 well from the north coastal aquifer during the dry season (summer). In this same dry season, $rCl/rHCO_3$ and rMg/rCa ratios in groundwaters from the middle part of the aquifer were 1.54 and 1.55, respectively.

During the winter rainy season, the $rCl/rHCO_3$ ratios show a seasonal maximum of 10.3 in well P2 in the north coastal aquifer. The rMg/rCa ratio shows a value of 1.86 in well P4 of the north coastal aquifer, and a ratio of 1.46 in well P10 of the southern coastal aquifer. Finally, the rNa/rCl ratio shows a value of 0.54 in well P2 from the north coastal aquifer, whereas wells P10 and P3 from the southern coastal aquifer exhibit higher ratios of 0.96 and 1.03, respectively. The Del Sauce stream in its lower section shows a rNa/rCl ratio of 0.18.

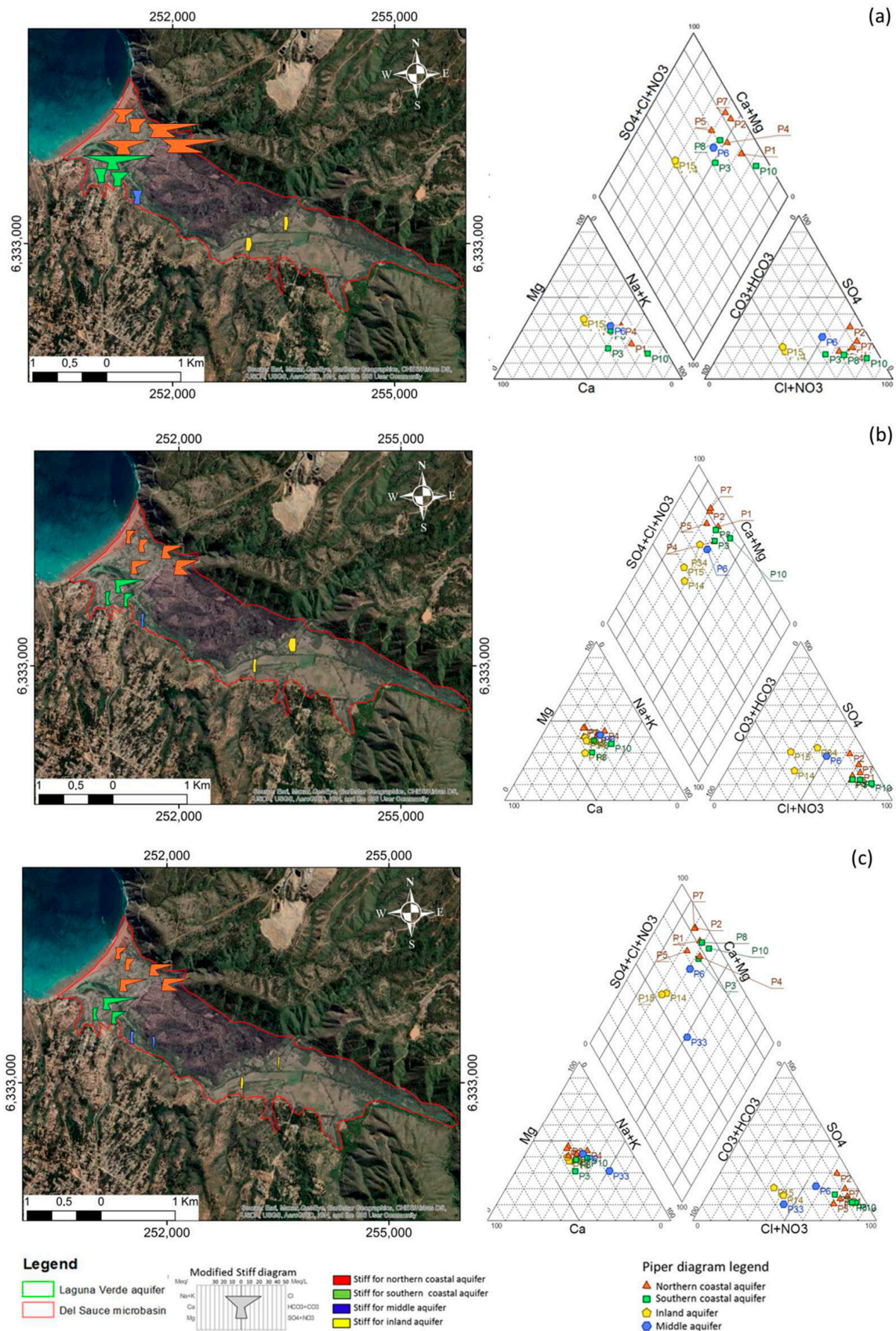


Figure 7. Cont.

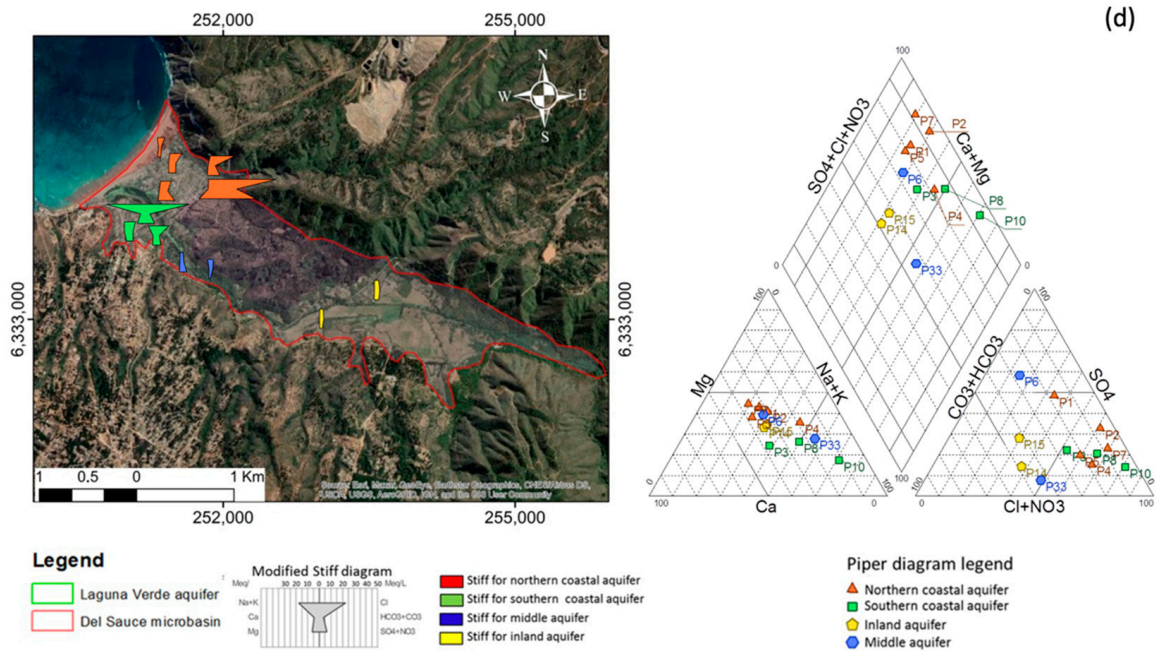


Figure 7. Laguna Verde aquifer hydrochemical maps, modified Stiff (left) and Piper (right) diagrams, for seasons: (a) spring 2021; (b) summer 2022; (c) autumn 2022; (d) winter 2022.

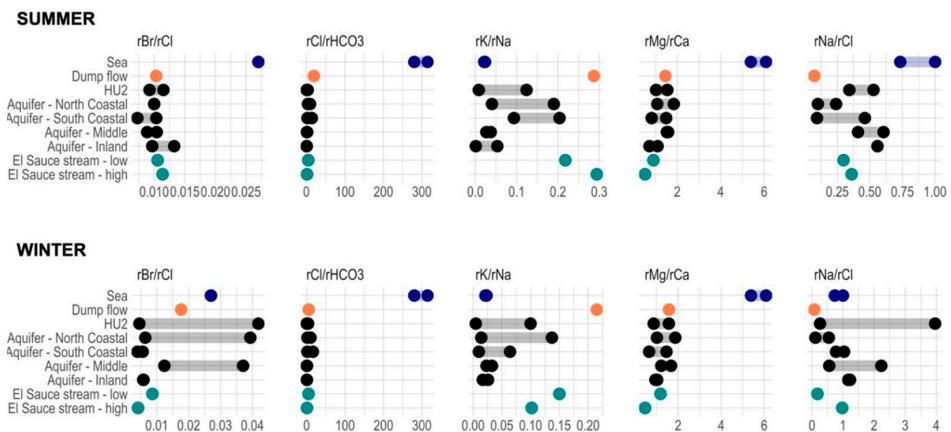


Figure 8. Comparative plot between ionic ratios of the studied hydric system. Superficial waters are highlighted in color and groundwaters are represented in black.

3.4.5. Isotopic Analysis

We observed a correlation between the waters of the estuary–aquifer system and the global meteoric water line (Figure 9). The superficial waters of the mainstream are lighter than the groundwaters of the aquifer. These waters were found to be more depleted in $\delta^{18}\text{O}$ ‰ and $\delta^2\text{H}$ ‰ in the highest sector (Las Cenizas; P20), with -10.4 $\delta^{18}\text{O}$ ‰ and -79.7 $\delta^2\text{H}$ ‰, and it is gradually enriched until the lower zone (lower El Sauce; S25), already close to its mouth, where averages of -7.3 $\delta^{18}\text{O}$ ‰ and -58.3 $\delta^2\text{H}$ ‰ were recorded. During the 2022 sampling, a gradual decrease of $\delta^{18}\text{O}$ ‰ and of $\delta^2\text{H}$ ‰ was observed since the summer season, where a maximum average of -7.3 $\delta^{18}\text{O}$ ‰ and -61.5 $\delta^2\text{H}$ ‰ V SMOW is recorded in these waters, until winter with an average of -9.8 $\delta^{18}\text{O}$ ‰ and -70.9 $\delta^2\text{H}$ ‰ V SMOW. In spring 2021, mean values were -9.2 $\delta^{18}\text{O}$ ‰ and -71.6 $\delta^2\text{H}$ ‰ V SMOW.

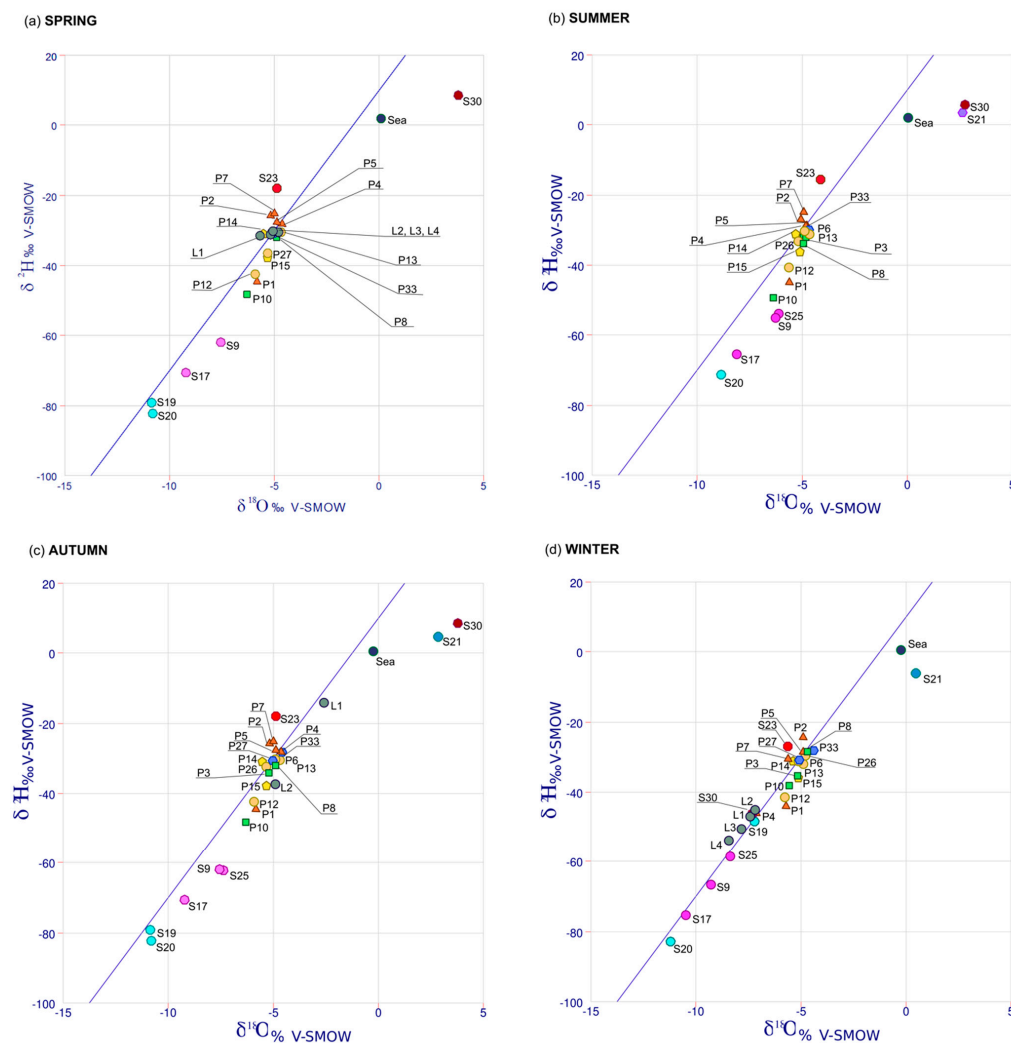


Figure 9. Diagrams of water isotopes $\delta^{18}\text{O}$ ‰ and $\delta^2\text{H}$ ‰ V SMOW for the total waters sampled in the four sampling campaigns: (a) spring, (b) summer, (c) autumn, (d) winter. In blue, global meteoric water line (GMWL).

Regarding the groundwaters of the Laguna Verde aquifer, the values are more similar to those of precipitation than to those of the main stream. The rainwater collected and analyzed showed values between -4.81 and -8.41 of $\delta^{18}\text{O}$ ‰ V SMOW and between -30.3 and -53.89 of $\delta^2\text{H}$ ‰ V SMOW, matching those of the GMWL. In groundwater, $\delta^{18}\text{O}$ data showed a low dispersion of data during the year (i.e., values between -4.65 and -7.11 $\delta^{18}\text{O}$ ‰ V SMOW, averaging -5.64 $\delta^{18}\text{O}$ ‰ V SMOW). However, $\delta^2\text{H}$ showed higher variability with values between -21.9 and -49.33 (average = -35.64 $\delta^2\text{H}$ ‰ V SMOW; Figure 9). On one hand, the sites the most depleted in both indicators correspond to P1, P10, and P15, showing characteristics of possible evaporation, because they are located slightly below the Global Meteoric Water Line GMWL [56–58]. On the other hand, the water samples of the aquifer corresponding to P7 and P2 are recognized for being located above the Global Meteoric Water Line and with the highest $\delta^2\text{H}$ ranges of the aquifer (annual averages of -26.5 and -25.7 $\delta^2\text{H}$ ‰ V SMOW, respectively).

While HU2 has a stable behavior throughout the year, well P12 robustly showed an isotopic signature similar to that of well P1 from the north coastal aquifer, with evidence of evaporation (i.e., slight enrichment in deuterium). Regarding the points associated with spills, the dump flow (S23) presents annual mean values of -4.9 $\delta^{18}\text{O}$ ‰ and -19.6 $\delta^2\text{H}$ ‰, while S30 records 0.7 $\delta^{18}\text{O}$ ‰ and -5.8 $\delta^2\text{H}$ ‰ V SMOW.

4. Discussion

Water scarcity in coastal areas is rising due to the increase in land occupation in these attractive zones. The increasing need for water generates significant pressures on the physical environment, especially on surface and subterranean water, which causes alterations to the natural environment. To carry out suitable hydric management, it is necessary to have a complete knowledge of the environment and of the relationships between water bodies. However, sufficient information is not always available, and in the specific case of the Laguna Verde locality (Valparaíso, Chile), there is hardly any data on the groundwater behavior and its relationship with surface water.

Based on the analysis and interpretation of the hydrological background and the collection of hydrodynamic, hydrochemical, and isotopic data, a conceptual model of the functioning of the Del Sauce wetland–Laguna Verde aquifer hydric system is proposed (Figure 10). The valley through which the Del Sauce stream flows constitute a small detritic aquifer whose main recharge is rainwater [21], while discharge into the sea can occur when the sandbar is opened. Precipitation during 2010–2022 shows the effects of the Mega-Drought that affected this area of the country, whereby precipitation was reduced by a mean of 25%, with occasional losses of 75%, as occurred in 2019 when only 130 mm was received [35]. During the last few years, the Del Sauce stream presented average flows of $0.26 \text{ m}^3/\text{s}$, coming from the Las Cenizas affluent. The isotopic signature of the stream waters confirmed that the water from the La Luz reservoir, which is much heavier due to evaporation processes, does not reach the Del Sauce stream, nor does the water from the artificial lagoon S30, which is strongly affected by pollution from the sanitary landfill. The flow values recorded during this study cannot be compared with data prior to the Mega-Drought as there are no previous records; however, hydrometric backgrounds in discharge zones of other natural channels in Central Chile indicate that these values would be reduced by up to 90% of the expected normal value [23].

From the piezometric information, significant anomalies are those shown in the sectors where wells P2 and P6 are located, as they present higher levels than the rest of the catchments. These could be related to possible water transfer areas from the lateral edges to the Laguna Verde aquifer.

Regarding the relationship of the Del Sauce stream with the Laguna Verde detritic coastal aquifer, everything indicates that in the inland zone (high Sauce, upstream), it behaves as a gaining river throughout the year (aquifer provides water to the stream) until it nears points P15 and P14, where the extraction of large water volumes alter this dynamic and cause a descent cone. It is more complex to establish the hydraulic relationship in the middle zone. As mentioned above, the existence of a possible recharge edge in its southern part makes it easier for the stream (middle Sauce) to behave as a gaining river, although pumping at point P33 could affect this relationship. Finally, in the coastal zone, the estuary behaves mainly as a losing stream, and it only occasionally receives some groundwater contributions. This behavior is not very usual, since the wetlands connected to the aquifers tend to feed them in rainy seasons, while in dry seasons, the opposite process occurs. However, the estuary that forms this wetland is dammed by a sandbar for most of the year, breaking up naturally in rainy seasons, which generates an increase in surface runoff water in dry seasons, and a decrease at certain times when the passage to the sea is opened in winter.

The isotopic signatures of the water wells P1 and P10, both located on both sides of the estuary, are somewhat more depleted than the other points of the aquifer in the coastal zone. This could be due to the mixing of the aquifer waters with the infiltrated waters coming from the humid zone.

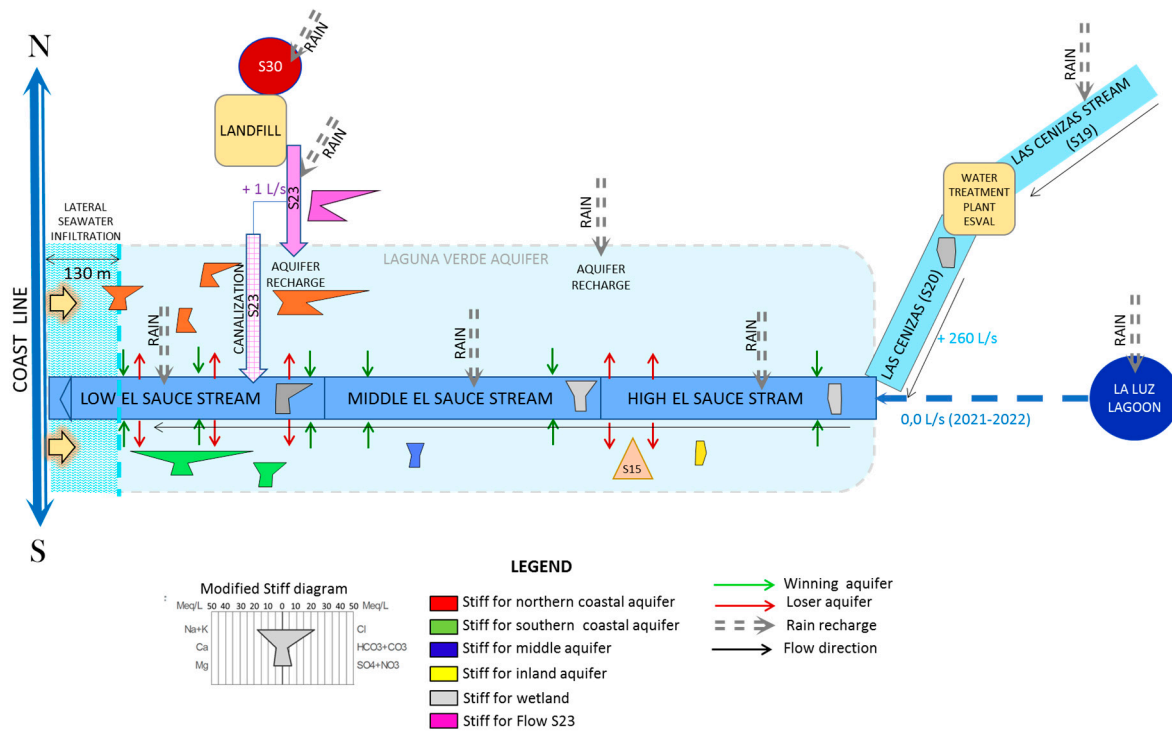


Figure 10. Conceptual hydrogeological–hydrogeochemical model of the Del Sauce wetland–Laguna Verde aquifer hydric system. Schematic plan view.

However, the different uncertainties mentioned above should be verified with longer piezometric monitoring and a higher number of sites. Bianchi et al. [59] and Schiavo et al. [60] suggested the use of stochastic simulations using the Monte Carlo method to capture the inherent variability of aquifer systems by generating multiple scenarios. Given that the available data come from a few wells and the column information shows variable and heterogeneous lithological characteristics, the best approach to establish a good conceptual model is through a stochastic model. Geostatistical methods, which are less demanding as they require little information, based on an estimated structural model with its uncertainty, have been applied with good results in heterogeneous detrital aquifers similar to those of Laguna Verde. We hereby provide the first step of a longer monitoring that will allow, with the use of these powerful models, the efficient assessment of the uncertainty in the geological and piezometric data.

In general, the stream waters vary from bicarbonate to (weakly) chloride in its upper course, with low mineralization, to chloride and sulfate waters with greater mineralization in the mouth zone, and with a progressive increase in nitrates concentration. All this causes the quality to deteriorate downstream. It is noted that the estuary waters have a certain salinity throughout their length and are not recommended for irrigation. This coincides with previous studies in which they were classified as poor-quality waters [28,31]. In its final section, the presence of fecal coliforms was also detected.

Groundwater presents a hydrodynamic and hydrochemical behavior similar to that of the stream waters. Broadly speaking, the water flow is from SW to NE, which is locally altered by the pumping effects. The chemical composition of its waters shows that the dominant facies in the inland part of the aquifer is bicarbonate, while the proportion of salts increases toward the coastal zone, with chloride becoming dominant. Another noteworthy characteristic is the presence of fecal coliforms in the coastal zone. This analysis shows the gradual deterioration of the water system from its source to the area closest to the coast, where high values of chlorides (440 mg/L) and nitrates (9.7 mg/L) stand out in the estuary, and with high values of chlorides (807 mg/L) and nitrites (57 mg/L), as well as Br (18 mg/L), in the aquifer. The highest values in the entire water system were retrieved from

runoff S23, which comes from the landfill and delivers its water to the coastal zone with annual averages of chloride and sulfates of 1987 and 1640 mg/L, respectively, 155 mg/L of nitrates and 59.4 mg/L of bromine.

All this indicates that in the coastal zone, both groundwater and surface water are affected by anthropic pollutant sources. First, the most important pollutant source corresponds to the flow coming from the vicinity of the sanitary landfill in the coastal zone (S23), which has notoriously high annual averages in relevant parameters (e.g., TDS, COD, sulfates, chlorides, nitrates, potassium), including the presence of coliforms; all these parameters are in ranges that some authors associate with leachates from sanitary landfills [61]. Their influence on groundwater seems clear because an elevation of the piezometric surface is generated in the environment of the discharge and there is a significant influence on the water quality near the discharge (wells P2 and P7). Also, the values of the ionic ratios $rCl/rHCO_3$ or rMg/Ca showed a similarity with those of the waters of this discharge, and the waters near the discharge present similar isotopic signatures. Finally, this water coming from the upper zone flows through a ravine of an E–W direction that has previously been interpreted as an inferred fault in the intrusive rock unit [43]. Therefore, it is not ruled out that this fluid may also infiltrate in some percentage along its route and flow into the aquifer subsurface through HU2 if the fault is considered to behave hydraulically as conductive, a behavior generally expected in 70% of faults, and in 60% of faults in crystalline rocks [62].

Secondly, the smaller-scale agricultural and livestock industries present in the inland and middle zone of the watershed (avocado plantations, cattle ranches, and alfalfa plantations in the inland zone of the basin; and small-scale crops in the middle zone) are considered another source of pollution. This pollution is detected by the progressive increase of up to 50 times more nitrates in the coastal zone of the aquifer compared to the inland zone. Such behavior is not observed in the surface water of the wetland, which has nitrates in similar concentrations throughout its length, which is interpreted as a direct infiltration of nitrogenous elements from the unsaturated zone into the aquifer, mainly as a result of agricultural and livestock activities in the upper and middle zone of the basin, where these industries are located. This is consistent with the EEA (2023) [63], which recognizes that mineral fertilizers and manure are the main sources of nitrate concentrations in groundwater in the EU, and it is estimated that 80% of the nitrogen spill to the aquatic environment in the EU comes from agriculture.

Finally, another source of pollution may correspond to raw wastewater and septic tank liquid discharged mainly in the populated area, affecting the saturated zone of the aquifer and the Del Sauce stream in its coastal zone. Based on the Metcalf and Eddy (1995) classification [64], this coastal sector presents high levels of wastewater indicators such as the presence of fecal coliforms throughout the year (up to 350 MPN/100 mL), maximum chloride and sulfate concentrations of 660 mg/L and 225 mg/L, respectively, and high TDS contents (annual mean of 1263 mg/L). This type of pollution is also detected in the Las Cenizas affluent, in the locality of Placilla, upstream of the water treatment plant (S19), recognized by the significant presence of fecal coliforms (>1000 MPN/100 mL), TDS annual mean of 637 mg/L, and high sulfate and chloride concentrations. The lack of infrastructure for the management of wastewater in the aquifer zone has led to the accumulation of pollutants in water bodies, which negatively affects public health and the environment, and shows the need to implement an adequate sanitation system.

In general, ionic relations, such as $rCl/rHCO_3$, rBr/Cl , or rMg/Ca , do not seem to show values that make us suspect a generalized marine intrusion in the aquifer. However, a salinity anomaly was observed near the estuary and other specific sites (i.e., P3, P4, and P10) whose ionic ratios are elevated at certain times and could point to some influence of seawater. In winter, storms and rough waters increase in the study area, a sector that has been classified as having a medium-to-high sensitivity or susceptibility to suffer floodings on the coastal edge due to storm surges. Other authors have assigned these processes as responsible for the mixing of fresh and saltwater [65–73].

When the sandbar that during a large part of the year dams the waters of the Del Sauce estuary opens in the sector of its mouth, the surface seawater intake occurs through the estuary, affecting its waters, which in turn infiltrates the nearest areas of the aquifer (i.e., P10). During the dry season (summer), a time of low aquifer recharge, it was detected that the rMg/rCa ionic ratio shows in P4 a ratio of 1.84, a value that is only attributable to a mixing with seawater. This seawater inflow possibly takes place from the coastline to at least 140 m inland (P4), laterally through the sandy sediments present in the coastal strip, an expected event in this type of aquifer [74], and/or horizontally because of flooding due to storm surge events.

The shallow depth of the piezometric level, the increase in rough waters and storms in recent years, and the increase in the population that uses the hydric resource in the Laguna Verde locality, together with the impact of pollutant sources, have reduced the freshwater availability for the populations and ecosystems in this coastal area. And this coincides with the findings reported by the IPCC [19], as this sector is very sensitive to the possible effects of climate change. The above exacerbates the relevance of employing suitable hydric resource management, where the basin as a territorial geographic unit is the most appropriate for the planning and management of water quality [17]. One of the most important management factors is the allocation of sufficient water of a quality suitable for the population and for maintaining the functions of the wetland ecosystems to be conserved. This requires consideration and management of land-based activities that affect coastal wetlands, such as commercial agriculture (which reduces available runoff in the headwaters of the basin), the damages caused to riparian areas (which alter the flow configuration and erosion/deposition patterns), and the extraction of an excessive groundwater volume (which can lower the phreatic zone and thus reduce the baseflow for wetlands and terrestrial ecosystems) [13]. This raises the need to obtain resources from other sources, such as desalination. The intake of seawater and brackish water through the ground, if feasible, presents favorable aspects, since they are susceptible to producing freshwater by membrane processes (desalting) at a lower production cost than seawater desalination [75]; therefore, it is of interest to promptly assess the possible extraction of these waters from the coastal aquifer, associating it with its possible environmental effects.

5. Conclusions

In the coastal region of Central Chile, the physical, hydrochemical, and isotopic analyses have been complementary in achieving a general and specific view of the behavior and quality of a wetland–aquifer hydric system. Under a climatic context of Mega-Drought in a Mediterranean climate, the quality of the hydric resource in the study area is recognized to be very deteriorated. Given the hydraulic connection, the specific pollutant sources have affected both the wetland and the estuary. These sources correspond mainly to the flow from the sanitary landfill and the one generated by the agricultural and livestock industries settled in the valley, in addition to slight seawater intrusion in some specific coastal sectors, which has increased the salinity in this area. This study provides unprecedented information about the physical, hydrometric, hydraulic, and hydrochemical characteristics of a coastal wetland–aquifer hydric system in central Chile, and the effects of its hydraulic connection. It contributes to a better understanding of the hydric dynamics and salinization processes in a coastal sector affected by anthropic pollution, raising concerns about the poor state of conservation of both surface water and groundwater resources, mainly in the coastal sector. We raised the need for integrated management of the sector's hydric resources that internalizes climatic variability, not allowing the direct use of these waters by the population, working on the reduction and elimination of the detected anthropic pollutant sources, and developing strategies for the recovery of the waters of the Del Sauce wetland and the Laguna Verde aquifer.

Supplementary Materials: The following supporting information can be downloaded at: <https://www.mdpi.com/article/10.3390/hydrology11100174/s1>. Table S1. Detailed list of methods used for physiochemical parameter measurements. Detection limit and accuracy are given. Figure S1. Riverside diagrams (USDA, 1975) for all samples of the hydric system in summer 2022 (left) and winter 2022 (right).

Author Contributions: Conceptualization, B.G., J.M.A.R., C.A.S. and C.L.; methodology, B.G., P.D., C.R., C.A.S. and C.L.; formal analysis, B.G., P.D. and C.L.; validation, J.M.A.R., C.A.S. and C.L.; investigation, B.G., A.B., S.F., A.Á. and C.L.; resources, C.A.S.; data curation, B.G., S.F. and C.L.; writing—original draft preparation, B.G.; writing—review and editing, J.M.A.R., C.A.S. and C.L.; visualization, B.G. and C.L.; supervision, C.A.S. and C.L.; project administration, C.A.S. and C.L.; funding acquisition, B.G., C.A.S. and C.L. All authors have read and agreed to the published version of the manuscript.

Funding: This work has been funded by the Sacyr (Chile and Spain), the FIC-R BIP project grant number 40046077 of the Regional Government of Valparaíso, and by the DGI Project of the Playa Ancha University, grant number CNE 16–20, awarded by D.E. No. 0345/2020, directed by Jean Pierre Francois. Céline L. was funded by the projects ANID InES I + D 2021 grant number INID210013 and Marie Curie Postdoctoral Fellowship HORIZON-MSCA-2022-PF-01 project grant number 101106387.

Data Availability Statement: The original contributions presented in the study are included in the article Supplementary Materials; further inquiries can be directed to the corresponding author.

Acknowledgments: We would like to thank the ideas and logistic support of Domingo Zarzo and Iván Sola. Also, we acknowledge the Laguna Verde community, who made it possible to gather the information presented in this study, mostly represented by Julia Poblete. We would also like to highlight the support we received from the president of the Laguna Verde APR, Colville Smith, to carry out this research. We acknowledge in this instance the technical and human support of the personnel that integrates the HUB Ambiental laboratory of the Playa Ancha University, mainly Fabiola Moenne as well as Sebastián Martorell, who also supported us as a specialist in environmental water sampling. We are grateful for the cooperation of the Stable Isotope Laboratory of the Alfred Wegener Institute (AWI) for Polar and Marine Research, Research Unit Potsdam for the measurement of water isotopes. Finally, we thank the ‘Support Network for the Review and Editing of Manuscripts’ of the Playa Ancha University. This work acknowledges the Severo Ochoa Centre of Excellence accreditation (CEX2019-000928-S) funded by AEI 10.13039/501100011033.

Conflicts of Interest: The authors declare no conflicts of interest.

References

1. Wörman, A.; Packman, A.I.; Marklund, L.; Harvey, J.W.; Stone, S.H. Fractal topography and subsurface water flows from fluvial bedforms to the continental shield. *Geophys. Res. Lett.* **2007**, *34*, L07402. [CrossRef]
2. Ramsar. The Ramsar Convention: What’s It All about? Secretaría de la Convención Ramsar 2015. Available online: https://www.ramsar.org/sites/default/files/fs_6_ramsar_convention.pdf (accessed on 15 January 2024).
3. Mitsch, W.J.; Gosselink, J.G. *Wetlands*, 2nd ed.; Van Nostrand Reinhold: New York, NY, USA, 1994.
4. Brinson, M.M.; Malvárez, A.I. Temperate freshwater wetlands: Types, status, and threats. *Environ. Conserv.* **2002**, *29*, 115–133. [CrossRef]
5. Finlayson, C.M. Forty years of wetland conservation and wise use. *Aquat. Conserv. Mar. Freshw. Ecosyst.* **2012**, *22*, 139–143. [CrossRef]
6. Davidson, N.C. How much wetland has the world lost? Long-term and recent trends in global wetland area. *Mar. Freshw. Res.* **2014**, *65*, 934–941. [CrossRef]
7. Gardner, R.C.; Barchiesi, S.; Beltrame, C.; Finlayson, C.; Galewski, T.; Harrison, I.; Paganini, M.; Perennou, C.; Pritchard, D.; Rosenqvist, A.; et al. *State of the World’s Wetlands and Their Services to People: A Compilation of Recent Analyses (March 31, 2015)*; Ramsar Briefing Note No. 7; Ramsar Convention Secretariat: Gland, Switzerland, 2015. [CrossRef]
8. Gardner, R.C.; Finlayson, C.M. *Global Wetland Outlook: State of the World’s Wetlands and Their Services to People*; Ramsar Convention Secretariat: Gland, Switzerland, 2018.
9. Xu, X.; Xiong, G.; Chen, G.; Fu, T.; Yu, H.; Wub, J.; Liu, W.; Su, Q.; Wang, Y.; Liu, S.; et al. Characteristics of coastal aquifer contamination by seawater intrusion and anthropogenic activities in the coastal areas of the Bohai Sea, eastern China. *J. Asian Earth Sci.* **2021**, *217*, 104830. [CrossRef]
10. Kazezyilmaz-Alhan, C.M. Analytical solutions for contaminant transport in streams. *J. Hydrol.* **2008**, *348*, 524–534. [CrossRef]
11. U.S. EPA. *Connectivity of Streams and Wetlands to Downstream Waters: A Review and Synthesis of the Scientific Evidence (Final Report)*; EPA/600/R-14/475F; U.S. Environmental Protection Agency: Washington, DC, USA, 2015.

12. Drexler, J.Z.; Knifong, D.; Tuil, J.L.; Flint, L.E.; Flint, A.L. Fens as whole-ecosystem gauges of groundwater recharge under climate change. *J. Hydrol.* **2013**, *481*, 22–34. [CrossRef]
13. Ramsar Convention Secretariat. *The Ramsar Convention Manual: A Guide to the Convention on Wetlands (Ramsar, Iran, 1971)*, 6th ed.; Ramsar Convention Secretariat: Gland, Switzerland, 2013.
14. Sophocleus, M. Interactions between groundwater and surface water: The state of the science. *Hydrogeol. J.* **2002**, *10*, 52–67. [CrossRef]
15. Ramsar. Humedales: En Peligro de Desaparecer en Todo el Mundo. Convención Sobre Humedales. Ficha Informativa 3. 2011. Available online: www.ramsar.org/es/acerca-de/uso-racional-de-los-humedales (accessed on 15 January 2024).
16. Xu, T.; Weng, B.; Yan, D.; Wang, K.; Li, X.; Bi, W.; Li, M.; Cheng, X.; Liu, Y. Wetlands of international importance: Status, threats, and future protection. *Int. J. Environ. Res. Public Health* **2019**, *16*, 1818. [CrossRef]
17. Stehr, A.; Álvarez, C.; Álvarez, P.; Arumí, J.L.; Baeza, C.; Barra, R.; Berroeta, C.A.; Castillo, Y.; Chiang, G.; Cotoras, D.; et al. Recursos hídricos en Chile: Impactos y adaptación al cambio climático. Informe de la mesa Agua. Santiago: Comité Científico COP25; Ministerio de Ciencia, Tecnología, Conocimiento e Innovación. 2019. Available online: https://cdn.digital.gob.cl/filer_public/e6/ff/e6ff260a-d926-4210-83e6-ad7b840b320c/19agua-recursos-hidricos-stehr.pdf (accessed on 15 January 2024).
18. IPCC. *Climate Change 2013: The Physical Science Basis. Contribution of Working Group I to the Fifth Assessment Report of the Intergovernmental Panel on Climate Change*; Cambridge University Press: Cambridge, UK, 2013.
19. IPCC. *Climate Change 2008: Impacts, Adaptation and Vulnerability. Contribution of Working Group II to the Fourth Assessment Report of the Intergovernmental Panel on Climate Change*; Cambridge University Press: Cambridge, UK, 2008.
20. Horton, B.P.; Rahmstorf, S.; Engelhart, S.E.; Kemp, A.C. Expert assessment of sealevel rise by AD 2100 and AD 2300. *Q. Sci. Rev.* **2014**, *84*, 1–6. [CrossRef]
21. Dirección General de Aguas (DGA). Inventario de Cuencas, Subcuencas y Subsubcuencas de Chile. DGA. División de Estudios y Planificación. 2014. Available online: <https://bibliotecadigital.ciren.cl/handle/20.500.13082/32709> (accessed on 25 October 2023).
22. Ministerio del Medio Ambiente de Chile (MMA). *Estrategia Nacional de Humedales 2024*; Ministerio del Medio Ambiente de Chile: Santiago, Chile, 2024.
23. CR2. Centro de Ciencia del Clima y la Resiliencia (CR2). *La Mega Sequía 2010–2015: Una Lección para el Futuro*; Informe a la Nación; CR2. Centro de Ciencia del Clima y la Resiliencia (CR2): Santiago, Chile, 2015.
24. Garreaud, R.D.; Boisier, J.P.; Rondanelli, R.; Montecinos, A.; Sepúlveda, H.H.; Veloso-Aguila, D. The Central Chile Mega Drought (2010–2018): A climate dynamics perspective. *Int. J. Climatol.* **2019**, *40*, 421–439. [CrossRef]
25. Masotti, I.; Aparicio-Rizzo, P.; Yevenes, M.A.; Garreaud, R.; Belmar, L.; Fariás, L. The Influence of River Discharge on Nutrient Export and Phytoplankton Biomass Off the Central Chile Coast (33°–37°S): Seasonal Cycle and Interannual Variability. *Front. Mar. Sci.* **2018**, *5*, 423. [CrossRef]
26. Dirección General de Aguas (DGA). Información Pluviométrica, Fluviométrica, Estado de Embalses y Aguas Subterráneas. Boletín N° 524 Mes Diciembre Año 2021. División de Hidrología (DGA). 2021. SSD: 15614003. Available online: https://dga.mop.gob.cl/productosyservicios/informacionhidrologica/Informacin%20Mensual/Boletin_12_Diciembre_2021.pdf (accessed on 26 July 2023).
27. Zúñiga, M. Caracterización de la Vulnerabilidad Socio Territorial en el área Rural, Forestal y de Expansión Urbana de Laguna Verde, Valparaíso. Bachelor's Thesis, Departamento de Geografía, Facultad de Ciencias Naturales y Exactas, Universidad de Playa Ancha, Valparaíso, Chile, 2015.
28. Rivera Castro, C.A.; Letelier Pino, J.A.; Acevedo Pizarro, B.; Tobar Correa, T.D.P.; Loreto Torres Lepe, C.; Cataldo Figueroa, A.M.; Rivera Castro, M.Á. Water quality in the El Sauce Estuary, Valparaíso, Central Chile. *Rev. Int. De Contam. Ambient.* **2020**, *36*, 261–273. [CrossRef]
29. Millanir, N. Proyecto de Factibilidad de Instalación de Redes de Alcantarillado y Agua Potable Sector Curaumilla-Laguna Verde. Bachelor's Thesis, Departamento de Diseño y Manufactura, Universidad Técnica Federico Santa María, Viña del Mar, Chile, 2003. AES/02/2012; Caracterización de aguas, Sector Laguna Verde, Quinta Región. Silob Chile. Informe técnico preparado por el Departamento de Ingeniería Ambiental: Valparaíso, Chile, 2012; 18p.
30. Pozo-Solar, F.; Cornejo-D'Ottone, M.; Orellana, R.; Acuña, C.; Rivera, C.; Aguilar-Muñoz, P.; Lavergne, C.; Molina, V. Microbial and Biogeochemical Shifts in a Highly Anthropogenically Impacted Estuary ("El Sauce" Valparaíso). *Water* **2023**, *15*, 1251. [CrossRef]
31. DGA. *Dirección General de Aguas, Gobierno de Chile. Evaluación de los Recursos Subterráneos de las Cuencas Costeras de la Quinta Región*; Informe Técnico. Serie de Documentos Técnicos S.D.T. N° 201; Dirección General de Aguas, Ministerio de Obras Públicas: Santiago, Chile, 2005; 93p.
32. Tobar, T.; and Torres, C.L. Evaluación de la calidad del agua del estero El Sauce, Laguna Verde: Impacto y Consecuencias. Bachelor's Thesis, Facultad de Ciencias Naturales y Exactas, Universidad de Playa Ancha, Valparaíso, Chile, 2014; 175p.
33. DGA. *Dirección General de Aguas, Gobierno de Chile. Evaluación de los Recursos Subterráneos de las Cuencas Costeras de la V Región*; Informe Técnico. Departamento de Recursos Hídricos. S.D.T. N°130; Dirección General de Aguas, Ministerio de Obras Públicas: Santiago, Chile, 2002; 43p.
34. Dirección Meteorológica de Chile (DMC). 2024. Available online: <https://climatologia.meteochile.gob.cl/> (accessed on 26 July 2023).

36. Superintendencia de Servicios Sanitarios (SISS). Decreto Supremo N°90/2000 Establece Norma de Emisión para la Regulación de Contaminantes Asociados a las Descargas de Residuos Líquidos a Aguas Marinas y Continentales Superficiales. Ministerio Secretaría General de la Presidencia, Chile. 2000. Available online: <https://bcn.cl/2esfo> (accessed on 14 July 2024).
37. Reyes, A.; Ulises, F.; Carvajal, Y. *Guía Básica para la Caracterización Morfométrica de Cuencas Hidrográficas*; Universidad del Valle: Cali, Colombia, 2010; 139p, ISBN 9789587654011.
38. Villela, S.M.; Mattos, A. *Hidrología Aplicada*; McGraw-Hill do Brasil: Sao Paulo, Brazil, 1975; 245p.
39. Strahler, A.N. Quantitative analysis of watershed geomorphology. *Eos Trans. Am. Geophys. Union* **1957**, *38*, 913–920. [[CrossRef](#)]
40. Alcántara, J.L. Caracterización Hidromorfométrica de la Microcuenca Puyllucana-Baños del Inca-Cajamarca, Mediante la Aplicación de ArcGis. Universidad Nacional de Cajamarca. 2008. Available online: https://alicia.concytec.gob.pe/vufind/Record/RUNC_800c627c183b752bafd2bd6892033979/Details (accessed on 15 August 2023).
41. Rizo, R.; Romero, L.; Zeledón, J. *Caracterización Biofísica y Socioeconómica de la Microcuenca La Jabonera, Perteneciente a la Subcuenca del Río Estelí*; Universidad Nacional Autónoma de Nicaragua: Managua, Nicaragua, 2011.
42. Gana, P.; Wall, R.; Gutiérrez, A.; Yañez, G. *Mapa Geológico Del Área Valparaíso–Curacaví, Región de Valparaíso y Región Metropolitana*; Esc. 1:100.000. Mapas Geológicos N° 1; Servicio Nacional de Geología y Minería: Santiago de Chile, Chile, 1994.
43. Gana, P.; Wall, R.; Gutiérrez, A. *Mapa Geológico del área de Valparaíso–Curacaví, Regiones de Valparaíso y Metropolitana [en línea]*; Mapas Geológicos N°001; SERNAGEOMIN: Santiago de Chile, Chile, 1996.
44. Encinas, A.; Le Roux, J.; Buatois, L.; Nielsen, S.; Finger, K.; Fourtanier, E.; Lavenu, A. Nuevo esquema estratigráfico para los depósitos marinos mio-pliocenos del área de Navidad (33°00′–34°30′ S), Chile central. *Rev. Geológica De Chile* **2006**, *33*, 221–246. [[CrossRef](#)]
45. Keller, B.Y.; Martin, A. Estudio de la Actividad de la Falla Laguna Verde para Zonificación de usos Urbanos y sus Restricciones. In Proceedings of the Congreso Geológico Chileno, Puerto Varas, Chile, 4 August 2000; pp. 77–78.
46. Instituto Privado de Investigación Sobre Cambio Climático (ICC). *Manual de Medición de Caudales*; ICC: Santa Lucía Cotzumalguapa, Guatemala, 2017; 18p, ISBN 978-9929-8241-4-0. Available online: <https://icc.org.gt/wp-content/uploads/2023/03/064.pdf> (accessed on 15 August 2024).
47. Richards, L. *Diagnosis and Improvement of Saline and Alkali Soils*; USDA Handbook 60; US Department of Agriculture: Washington, DC, USA, 1954.
48. Instituto Nacional de Normalización (INN). *Norma Chilena Oficial NCh 1333/78. Modificada en 1987. Requisitos de Calidad del agua para Diferentes Usos*; Gobierno de Chile: Santiago, Chile, 1987.
49. Fundación Centro Internacional de Hidrología Subterránea (FCIHS). *Hidrogeología*; Fundación Centro Internacional de Hidrología Subterránea: Barcelona, Spain, 2009.
50. Piper, A.M. A graphic procedure in the geochemical interpretation of water-analyses. *Trans. Am. Geophys. Union* **1944**, *25*, 914–928.
51. Custodio, E.; Llamas, M.R. *Hidrología Subterránea*; Ediciones Omega, S. A.: Barcelona, Spain, 1976; 2350p.
52. López-Geta, J.A.; Mena, J.M. *Aspectos Metodológicos en el Estudio de la Intrusión Salina. Documento Básico*; Geomecánica y Aguas S.A. para División de Aguas Subterráneas y Geotécnica del Instituto Geológico y Minero de España: Madrid, Spain, 1988; 230p.
53. Giménez, E.; Morell, I. Análisis hidrogeoquímico de los procesos de salinización en el acuífero costero de Oropesa (Castellón, España). *Environ. Geol.* **1997**, *29*, 118–131. [[CrossRef](#)]
54. DGA. *Dirección General de Aguas, Gobierno de Chile. Estimación de la Demanda Actual, Proyecciones Futuras y Caracterización de la calidad de los Recursos Hídricos en Chile*; Unión Temporal de Proveedores Hídrica Consultores SPA y Aquaterra Ingenieros Ltda. S.I.T. N°419; Ministerio de Obras Públicas, Gobierno de Chile: Santiago, Chile, 2017.
55. Freeze, R.A.; Cherry, J.A. *Groundwater*; Prentice-Hall: Hoboken, NJ, USA, 1979; 604p.
56. Craig, H. Isotopic variations in meteoric waters. *Science* **1961**, *133*, 1702–1703. [[CrossRef](#)]
57. Dansgaard, W. Stable isotopes in precipitation. *Tellus* **1964**, *16*, 436–468. [[CrossRef](#)]
58. Gat, J.R. Oxygen and hydrogen isotopes in the hydrologic cycle. *Annu. Rev. Earth Planet. Sci.* **1996**, *24*, 225–262. [[CrossRef](#)]
59. Bianchi Janetti, E.; Riva, M.; Guadagnini, A. Natural springs protection and probabilistic risk assessment under uncertain conditions. *Sci. Total Environ.* **2021**, *751*, 141430. [[CrossRef](#)] [[PubMed](#)]
60. Schiavo, M. Entropy, fractality, and thermodynamics of groundwater pathways. *J. Hydrol.* **2023**, *617*, 128930. [[CrossRef](#)]
61. Aziz, O.I.; Burn, D.H. Trends and variability in the hydrological regime of the Mackenzie River Basin. *J. Hydrol.* **2006**, *319*, 282–294. [[CrossRef](#)]
62. Scibek, J.; Gleeson, T.; McKenzie, J.M. The biases and trends in fault zone hydrogeology conceptual models: Global compilation and categorical data analysis. *Geofluids* **2016**, *16*, 782–798. [[CrossRef](#)]
63. EEA. European Environment Agency. Europe’s Groundwater: A Key Resource under Pressure. Report. 2022. Available online: <https://www.eea.europa.eu/publications/europes-groundwater> (accessed on 5 July 2024).
64. Metcalf & Eddy, Inc. *Wastewater Engineering: Treatment, Disposal, and Reuse*; McGraw-Hill: New York, NY, USA, 1995.
65. Strack, O.D.L. A single-potential solution for regional interface problems in coastal aquifers. *Water Resour. Res.* **1976**, *12*, 1165–1174. [[CrossRef](#)]
66. Ataie-Ashtiani, B.; Volker, R.E.; Lockington, D.A. Tidal effects on sea water intrusion in unconfined aquifers. *J. Hydrol.* **1999**, *216*, 17–31. [[CrossRef](#)]
67. Levanon, E.; Yechieli, Y.; Haim, G.; Eyal, S. Tide-induced fluctuations of salinity and groundwater level in unconfined aquifers-field measurements and numerical model. *J. Hydrol.* **2016**, *551*, 665–675. [[CrossRef](#)]

68. Loáiciga, H.; Pingel, T.; Garcia, E. Sea Water Intrusion by Sea-Level Rise: Scenarios for the 21st Century. *Ground Water* **2012**, *50*, 37–47. [[CrossRef](#)]
69. Wang, J.; Tsay, T. Tidal Effects on Groundwater Motions. *Transp. Porous Media* **2001**, *43*, 159–178. [[CrossRef](#)]
70. Michael, H.; Mulligan, A.; Harvey, C. Seasonal oscillations in water exchange between aquifers and the coastal ocean. *Nature* **2005**, *436*, 1145–1148. [[CrossRef](#)] [[PubMed](#)]
71. Werner, A.D.; Simmons, C.T. Impact of sea-level rise on seawater intrusion in coastal aquifers. *Groundwater* **2009**, *47*, 197–204. [[CrossRef](#)]
72. Yechieli, Y.; Shalev, E.; Wollman, S.; Kiro, Y.; Kafri, U. Response of the Mediterranean and Dead Sea coastal aquifers to sea level variations. *Water Resour. Res.* **2010**, *46*, W12550. [[CrossRef](#)]
73. Ketabchi, H.; Mahmoodzadeh, D.; Ataie-Ashtiani, B.; Simmons, C. Sea-level rise impacts on seawater intrusion in coastal aquifers: Review and integration. *J. Hydrol.* **2016**, *535*, 235–255. [[CrossRef](#)]
74. Custodio, E. Coastal aquifers in Europe: An overview. *J. Hydrol.* **2010**, *18*, 269–280. [[CrossRef](#)]
75. Custodio, E.; Lázaro, M.; Martínez, R. Salinización de las aguas subterráneas en los acuíferos. *Rev. De La Soc. Española De Hidrogeol.* **2017**, *27*, 43–60.

Disclaimer/Publisher’s Note: The statements, opinions and data contained in all publications are solely those of the individual author(s) and contributor(s) and not of MDPI and/or the editor(s). MDPI and/or the editor(s) disclaim responsibility for any injury to people or property resulting from any ideas, methods, instructions or products referred to in the content.